AD-A080 604 SYRACUSE UNIV N Y DEPT OF ELECTRICAL ENGINEERING F/G 20/14
FEATURES STUDY - A STUDY OF RF EXTERNAL TRANSMISSIONS.(U)
NOV 79 J PERINI, B SIVERMAN, E NYAKABWA F30602-78-C-0083
UNCLASSIFIED RADC -TR-79-272 NL

| OF |
AD
A080604

END
DATE
FILMED
3 - 80
DDC

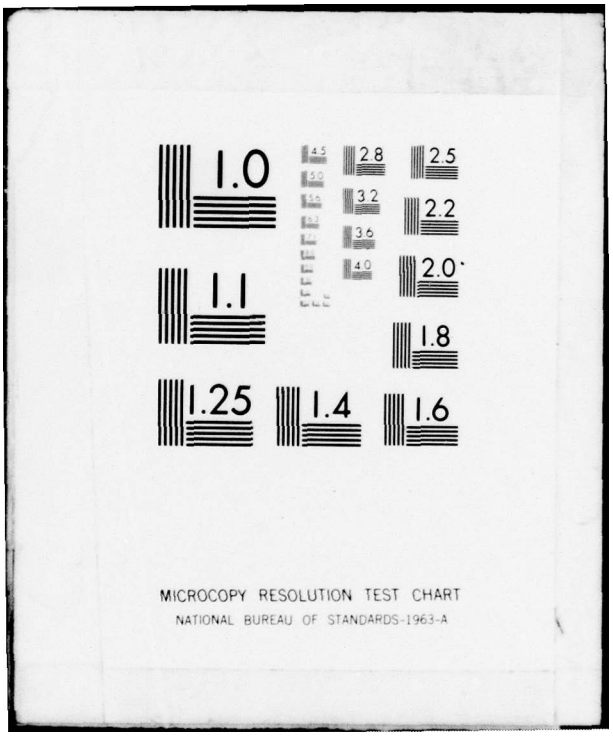
1.0
1.1
1.25
1.4
1.6
1.8
2.0
2.2
2.5
2.8
3.2
3.6
4.0
4.5
5.0
MICROCOPY RESOLUTION TEST CHART
NATIONAL BUREAU OF STANDARDS-1963-A

LEVEL II

RADC-TR-79-272
Final Technical Report
November 1979

FEATURES STUDY - A STUDY OF RF EXTERNAL TRANSMISSIONS

Syracuse University

Dr. J. Perini
Dr. B. Silverman
Mr. E. Nyakabwa

Laboratory Directors' Fund No. 01737814

ROME AIR DEVELOPMENT CENTER
Air Force Systems Command
Griffiss Air Force Base, New York 13441

This report has been reviewed by the RADC Public Affairs Office (PA) and is releasable to the National Technical Information Service (NTIS). At NTIS it will be releasable to the general public, including foreign nations.

RADC-TR-79-272 has been reviewed and is approved for publication.

APPROVED: Jeffrey N. Knieriemen

JEFFREY N. KNIERIEMEN, CAPT, USAF
Project Engineer

APPROVED: Howard Davis

HOWARD DAVIS
Technical Director
Intelligence & Reconnaissance Division

FOR THE COMMANDER: John P. Huss

JOHN P. HUSS
Acting Chief, Plans Office

This effort was funded totally by the Laboratory Directors' Fund

If your address has changed or if you wish to be removed from the RADC mailing list, or if the addressee is no longer employed by your organization, please notify RADC (IRAE), Griffiss AFB NY 13441.

Do not return this copy. Retain or destroy.

UNCLASSIFIED

SECURITY CLASSIFICATION OF THIS PAGE (When Data Entered)

REPORT DOCUMENTATION PAGE

READ INSTRUCTIONS BEFORE COMPLETING FORM

1. REPORT NUMBER: RADC-TR-79-272	2. GOVT ACCESSION NO.
3. RECIPIENT'S CATALOG NUMBER	
4. TITLE (and Subtitle): FEATURES STUDY - A STUDY OF RF EXTERNAL TRANSMISSIONS	5. TYPE OF REPORT & PERIOD COVERED: Final Technical Report 15 Oct 78 — 30 Jun 79
	6. PERFORMING ORG. REPORT NUMBER: N/A
7. AUTHOR(s): Dr. J. Perini; Dr. B. Silverman; Mr. E. Nyakabwa	8. CONTRACT OR GRANT NUMBER(s): F30602-78-C-0083
9. PERFORMING ORGANIZATION NAME AND ADDRESS: Syracuse University, Department of Electrical Engineering, Syracuse NY 13201	10. PROGRAM ELEMENT, PROJECT, TASK AREA & WORK UNIT NUMBERS: 61011F; 01737814; 78
11. CONTROLLING OFFICE NAME AND ADDRESS: Rome Air Development Center (IRAE), Griffiss AFB NY 13441	12. REPORT DATE: November 1979
	13. NUMBER OF PAGES: 78
14. MONITORING AGENCY NAME & ADDRESS (if different from Controlling Office): Same	15. SECURITY CLASS. (of this report): UNCLASSIFIED
	15a. DECLASSIFICATION/DOWNGRADING SCHEDULE: N/A

16. DISTRIBUTION STATEMENT (of this Report)

Approved for public release; distribution unlimited.

17. DISTRIBUTION STATEMENT (of the abstract entered in Block 20, if different from Report)

Same

18. SUPPLEMENTARY NOTES

RADC Project Engineer: Jeffrey N. Knieriemen (IRAE)

This effort was funded totally by the Laboratory Directors' Fund

19. KEY WORDS (Continue on reverse side if necessary and identify by block number)

Multipath Delay	Antenna Radiation Pattern
Signal Processing	RF Externals
Fast Fourier Transforms	Bistatic Echos
Cepstral Processing	Aircraft Configuration Analysis

20. ABSTRACT (Continue on reverse side if necessary and identify by block number)

Cepstrum and Fast Fourier Transform techniques are developed which provide a theoretical basis for determining the configuration of aircraft and space vehicles. Some of the limiting assumptions of the analysis, and possible problem areas are discussed.

The antenna radiation pattern of an "omnidirectional" antenna is largely determined by the shape, composition, location and size of the features of the vehicle to which the antenna is attached. The objective of this effort was to develop a method for determining the features and/or (Cont'd)

DD FORM 1 JAN 73 1473

UNCLASSIFIED

SECURITY CLASSIFICATION OF THIS PAGE (When Data Entered)

339 712

Item 20 (Cont'd)

configuration of an aircraft or space vehicle from signals transmitted by those vehicles. A signal processing technique called Cepstral Processing offered the best chance to do this. Cepstral Processing is based on the fact that an RF signal sensed in the far field of the transmitting antenna will be a complex composite of the direct antenna signal path, and multipath reflections from vehicle wing surfaces, landing gear struts, fuel pods, etc.

This report documents two possible approaches for extracting required feature information from omnidirectional signals. The first approach is Time Signal Processing. If the transmitter is producing a pulsed waveform (such as a data link signal) each pulse should contain the direct signal plus the attenuated delayed signals resulting from on-board reflectors (surfaces, wings, etc). Cepstral Processing can be applied to the RF, IF, or base band waveform with the result being a plot of the time delay and amplitude of each reflection. While this does not uniquely locate each reflector it does identify that the object location is on an elipse with the transmitter antenna and the receiving antenna being at the foci. Taking several aspect angles, these elipses will cross at a point and therefore fix the object position.

The second approach Antenna Radiation Pattern Processing. Here 90^{o} of aspect angle change is non-uniformly sampled in a manner consistent with the Cepstrum equations and again the result is a plot of time delay and amplitude of reflections.

While both approaches give the same type of output, they are complementary not redundant. For a specific situation one may be desired over the other. Both approaches appear feasible at this time, but future effort should investigate the effects of noise, digitization sampling rates, non-linearity of receivers, non-omnidirectional reflections, and object location ambiguity.

PREFACE

This effort was conducted by Syracuse University under the sponsorship the Rome Air Development Center Post-Doctoral Program for Rome Air elopment Center. Capt. Jeffrey Knieriemen, RADC/IRAE, was the task project ineer and provided overall technical direction and guidance.

The RADC Post-Doctoral Program is a cooperative venture between RADC some sixty-five universities eligible to participate in the program. acuse University (Department of Electrical Engineering), Purdue Univer- (School of Electrical Engineering), Georgia Institute of Technology ıool of Electrical Engineering), and State University of New York at alo (Department of Electrical Engineering) act as prime contractor ›ols with other schools participating via sub-contracts with prime ›ols. The U.S. Air Force Academy (Department of Electrical Engineering), Force Institute of Technology (Department of Electrical Engineering), the Naval Post Graduate School (Department of Electrical Engineering) participate in the program.

The Post-Doctoral Program provides an opportunity for faculty at icipating universities to spend up to one year full time on explora- development and problem-solving efforts with the post-doctorals tting their time between the customer location and their educational itutions. The program is totally customer-funded with current pro- ; being undertaken for Rome Air Development Center (RADC), Space and .le Systems Organization (SAMSO), Aeronautical System Division (ASD),

Electronics Systems Division (ESD), Air Force Avionics Laboratory (AFAL), Foreign Technology Division (FTD), Air Force Weapons Laboratory (AFWL), Armament Development and Test Center (ADTC), Air Force Communications Service (AFCS), Aerospace Defense Command (ADC), HQ USAF, Defense Communications Agency (DCA), Navy, Army, Aerospace Medical Division (AMD), and Federal Aviation Administration (FAA).

Further information about the RADC Post-Doctoral Program can be obtained from Mr. Jacob Scherer, RADC/RBC, Griffiss AFB, NY, 13441, telephone Autovon 587-2543, Commercial (315) 330-2543.

TABLE OF CONTENTS

EVALUATION

The Features Study Project was fully funded by the Rome Air Development Center Laboratory Director's Fund. Syracuse University has developed two unique approaches for deriving the features, characteristics, and configuration of airborne vehicles. These digital signal processing techniques utilize RF Transmissions from omnidirectional antennas on-board the target vehicle. The Transmissions are received and recorded by remotely located receiving systems. There are many questions still to be resolved, but this effort has provided basic research into an area of very high potential pay-off.

Jeffrey N. Knieriemen

JEFFREY N. KNIERIEMEN, CAPT, USAF
Project Engineer

1. INTRODUCTION

1.1 Objective

This study was motivated by an interest in determining features and characteristics of the configurations of aircraft and space vehicles by monitoring their RF external transmissions. The theoretical foundations are presented in this report, along with simulation results, from which techniques can be developed to implement this method of detection. Additional work is needed to determine whether or not the techniques are practically feasible.

1.2 Background

This was a theoretical study of limited time duration. A survey of the unclassified literature did not reveal any publications relating directly to this subject. Consideration of many of the existing detection techniques, such as those used in radar systems, did not suggest any methods of solution to this proposed problem. Finally, it was decided to concentrate this study on the application of Cepstrum* techniques to this problem.

2. GENERAL APPROACH - CEPSTRUM ANALYSIS

In the analysis that follows, it is assumed that the particular type vehicle which is being monitored has been identified and the objective is that of determining its configuration. In other words, can it be determined

---

*B.P. Bogert, M.J.R. Healy, and J.W. Tukey, "The Quefrency Analysis of Time Series for Echoes," Pro. Symp. Time Series Analysis, M. Rosenblatt, ed., John Wiley and Sons, N.Y., 1963, pp. 209-243.

if the known type vehicle is armed, are its wheels down, are its wing tanks in place, etc. The general approach to developing such a method of detection is as follows. It is assumed that the RF transmissions of any vehicle of interest has been monitored and recorded in the past when the vehicle is in what may be called a 'normal' or 'neutral' configuration. In the analysis below, this known signal is represented by $x(t)$. Any change in this normal configuration, such as the addition of armaments or wing tanks, will be equivalent to introducing obstacles or scatterers which will affect the patterns of the vehicle's transmitting antennas. In fact, these obstacles are interpreted as point sources of reflections which distort the original signals by causing multipath transmissions. Cepstrum analysis of this multipath signal provides an estimate of the locations of the reflections and, hence, an estimate of the change in the vehicle features.

For example, suppose that an aircraft has an omnidirectional antenna mounted under the fuselage as shown in Figure 1. Furthermore, assume that the far-field signal, $x(t)$, received from this antenna is known. To simplify the illustration assume that the aircraft is moving on a radial straight line toward the receiving site.

Now suppose that armament is placed under the wing as indicated in Figure 2. Under this condition, the received signal is:

$$y(t) = x(t) + \alpha x(t - \tau). \tag{1}$$

The distance d in Fig 2 is related to by:

$$d = c\tau, \text{ where } c \text{ is free-space velocity of propagation of the signal.} \tag{2}$$

For a given vehicle, if d is determined, its configuration is known; or,

NORMAL CONFIGURATION OF AIRCRAFT

FIGURE 1

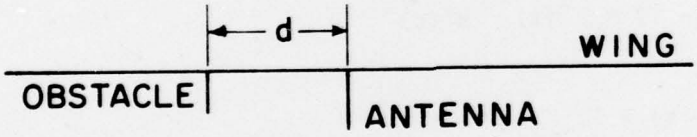

MODIFIED CONFIGURATION OF AIRCRAFT

FIGURE 2

in general, if locations of several sources of reflections are determined, information about the configuration of the vehicle is obtained.

A cepstrum analysis of (1) will now be developed to illustrate how τ and α can be determined.

Take the Fourier transform of (1):

$$Y(\omega) = X(\omega)[1 + \alpha\varepsilon^{-j\omega\tau}] \tag{3}$$

After this, take the logarithm of both sides:

$$\ell n(Y(\omega) = \ell n(X(\omega)) + \ell n[1 + \alpha\varepsilon^{-j\omega\tau}] \tag{4}$$

Assume $|\alpha| << 1$. Note: This assumption is not necessary, but it simplifies the analysis.* Then:

$$\ell n(Y(\omega)) = \ell n(X(\omega)) + \alpha\varepsilon^{-j\omega\tau} \tag{5}$$

Taking the inverse Fourier transform:

$$F^{-1}(\ell nY(\omega)) = y'(t) = F^{-1}(\ell nX(\omega)) + \alpha\delta(t - \tau)$$

$$= x'(t) + \alpha\delta(t - \tau) \tag{6}$$

$$\alpha\delta(t - \tau) = y'(t) - x'(t) \tag{7}$$

where

$$\delta(t - \tau) = 1, \quad t = \tau$$

$$= 0 \quad \text{elsewhere.}$$

Equation (7) is our desired result. Recall that x(t) and, consequently, $x'(t)$ are known. Also, y(t) is the received signal; therefore, $y'(t)$ is known. Therefore, (7) yields an impulse of strength α located

---

* $\ell n(1 + w) = w - \frac{w^2}{2} + \frac{w^3}{3} - \ldots = \sum_{n=1}^{\infty} (-1)^{(n+1)} \frac{w^n}{n}$; $w^2 < 1$

at $t = \tau$. But $d = c\tau$ and, therefore, d has been determined. This indicates that an object has been added to the vehicle at a distance, d, from the antenna as indicated in Figure 2. Note: If $|\alpha| << 1$ does not hold, equation (7) will include additional terms of the form $(-1)^{(n+1)}\frac{\alpha^n}{n} \cdot \delta(t - n\tau)$ which can be identified and disregarded.

This same analysis can be applied to cases of more than one source of reflections. Examples of multiple reflections are included in the simulation results.

There are a number of different ways in which this technique may be processed in practice. Two specific methods were selected for further development and computer simulation in the remaining time available. One method is that of processing the received RF signal directly as a time function. Because this implementation follows naturally from the cepstrum analysis presented above, it is developed first in this report. The other method monitors and processes the radiation pattern of the RF transmissions. It requires additional innovation and is presented second.

3. TIME SIGNAL PROCESSING

3.1 Analysis

A signal typical of what many aircraft may transmit is shown in Figure 3. It may be processed at the receiver as an RF, IF, or baseband signal. If the receiver does not distort the original multipath relations, it is convenient to process the baseband or envelope signal. As shown in what follows, processing the signal after it has passed through any linear filter, yields the same result.

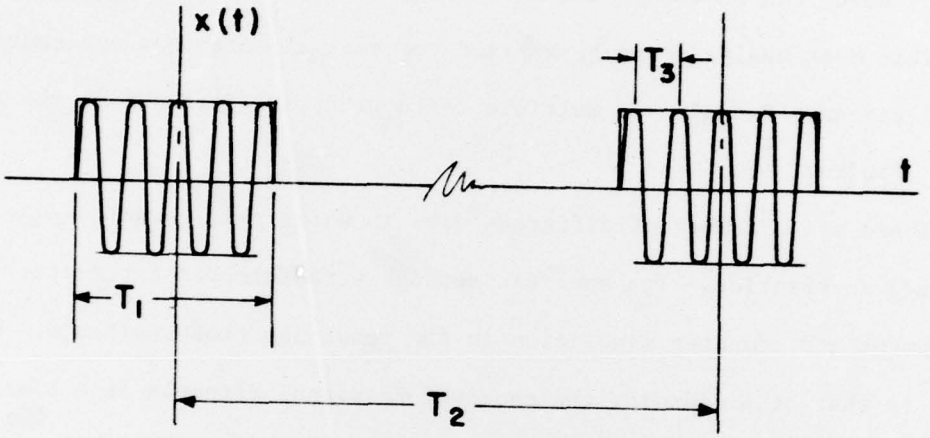

TYPICAL RF TRANSMISSION

$(T_1 = 1(10)^{-6}\,s;\ T_2 = 40(10)^{-6}\,s;\ f_c = \frac{1}{T_3} = 300(10)^6\,Hz)$

FIGURE 3

In practice, of course, this analysis would be accomplished on a digital computer using the discrete Fourier transform (DFT) or Fast Fourier Transform (FFT). Consequently, in the example below the signal is given as discrete data and numerical or discrete techniques are used.

The received signal is represented as:

$$y(n) = x(n) + \sum_{i=1}^{p} \alpha_i x(n - n_i). \tag{8}$$

In (8), x(n) is the received signal when the vehicle is in its 'normal' configuration and $\sum_{i=1}^{p} \alpha_i x(n - n_i)$ represents the contributions of p obstacles. The variable, time, has been suppressed and the interval (n(K+1) - n(K)) corresponds to the unit sampling time, T_s.

If y(n) is passed through a linear filter whose impulse response is h(n),

$$s(n) = y(n) * h(n) \tag{9}$$

where * indicates convolution. Note: Multiplication is represented by the symbol * in the computer printouts.

Taking the Fast Fourier Transform (FFT) of (9) yields:

$$S(K) = Y(K)H(K) = X(K)(1 + \sum_{i=1}^{p} \alpha_i e^{-j(2\pi/N)Kn_i})H(K) \tag{10}$$

where

$$Y(K) = \sum_{n=0}^{(N-1)} [x(n) + \sum_{i=1}^{p} \alpha_i x(n - n_i)]\varepsilon^{-j(2\pi/N)Kn} \quad ; \quad K = 0,1,2 \ldots (N-1) \tag{11}$$

$$H(K) = \sum_{n=0}^{(N-1)} h(n)\varepsilon^{-j(2\pi/N)Kn} \quad ; \; K = 0,1,2 \ldots (N-1) \tag{12}$$

Next:

$$\ell n|S(K)|^2 = \ell n|X(K)H(K)|^2 + \ell n|1 + \sum_{i=1}^{p} \alpha_i \varepsilon^{-j(2\pi/N)Kn_i}|^2 \qquad (13)$$

Here the $\ell n|S(K)|^2$ is used instead of $\ell n[S(K)]$ as indicated in Section 2. The logarithm of a complex number is multivalued. Usually, in computations only the principal value is used. When dealing with functions that vary over more than one wavelength, this practice introduces discontinuities and errors in the results. Using the magnitude or absolute value of S(K) eliminates this problem. However, in the result this introduces an impulse at $(N - n_i)$ as well as n_i when a signal $\alpha_i x(n - n_i)$ is present. This additional impulse can be recognized and disregarded as shown in the simulation below.

$$\text{If } |\alpha_i| << 1, \text{ i.e., } \alpha_m \alpha_\ell \simeq 0, \qquad (14)$$

$$\ell n|S(K)|^2 \simeq \ell n|X(K)H(K)|^2 + \sum_{i=1}^{p} 2\alpha_i \cos\left(\frac{2\pi}{N} n_i K\right)$$

$$\sum_{i=1}^{p} 2\alpha_i \cos\left(\frac{2\pi}{N} n_i K\right) \simeq \ell n|S(K)|^2 - \ell n|X(K)H(K)|^2 \qquad (15)$$

Applying the inverse FFT (FFT^{-1}):

$$\sum_{i=1}^{p} \alpha_i [\delta(n - n_i) + \delta(n + n_i)] = FFT^{-1} \ell n|S(K)|^2 - FFT^{-1} \ell n|X(K)H(K)|^2. \qquad (16)$$

Again, (16) is our desired result. Recall that X(K) is known because x(n) is known and S(K) is determined from y(n) which is the received signal. Note in (16) that there are two impulses for each reflection. Because of the periodicity of the FFT, $(n + n_i) = (N - n_i)$.

Also, if the condition $|\alpha_i| << 1$ does not apply, additional impulses are present. This is discussed below. Also note that any processing of the received signal that may be represented by a linear transfer function such as H(K) appearing with the above equations will not affect the results.

3.2 Simulation

This technique was simulated on a digital computer. The program, SILVERMAN/DRSIL, which was used is included in the appendix. The results are as predicted by the theory in these abstract, noiseless examples. Four cases are illustrated in Figures 5 through 25.

Case I: One Reflection

$x(n) = 1, \quad 0 \leq n \leq 7$ (Fig. 5)

$= 0, \quad 8 \leq n \leq 15$

$h(n) = \varepsilon^{-0.25n}$ (Fig. 7)

$\alpha = 0.2$

$n_i = 3$ (delay)

Figure 10 is a plot of the cepstrum: $\alpha_i[\delta(n - n_i) + \delta(n + n_i)] = 0.2[\delta(n - 3) - \delta(n + 3)]$. Note the amplitude of $\alpha = 0.2$ at $n = 3$ and $n = (N - 3) = 13$. Also note the amplitude $= (-0.1)\alpha = -0.02$ at $n = 6$ and $n = (N - 6) = 10$. These addition impulses occur because of the expression for the logarithm:

$$\ell n(1 + w) = w - \frac{w^2}{2} + \frac{w^3}{3} - \frac{w^4}{4} + \ldots \quad .$$

In the analysis in Section 2 it is assumed that $\ell n(1 + w) \simeq w$. In this particular case: $w = 2\alpha \cos(\frac{2\pi}{N} n_i K) = 0.4 \cos \frac{\pi}{8} (3K)$, and

$$-\frac{w^2}{2} = \frac{(0.4)^2}{2}\cos\left(\frac{\pi}{8}3K\right)^2 = (0.04)(1 - \cos\frac{\pi}{8}6K)$$

$$= -0.02[1 - \varepsilon^{j(\pi/8)6K} - \varepsilon^{-j(\pi/8)6K}]$$

This term accounts for the cepstrum responses at n = 6 and n = (N-6) = 10. Because only the magnitudes of the data are plotted, the minus sign is not apparent at n = 6 and n = 10, but it did appear in the numerical calculations.

Case 2. Two Reflections

$x(n) = 1, \quad 0 \leq n \leq 7$ (Fig. 11)

$= 0, \quad 8 \leq n \leq 15$

$h(n) = \varepsilon^{-0.25n}$ (Fig. 7)

$\alpha_1 = 0.2 \quad ; \alpha_2 = 0.1$

$n_1 = 3 \quad ; n_2 = 4$

Figure 15 is a plot of the cepstrum:

$$\alpha_1[\delta(n - n_1) + \delta(n + n_2)] + \alpha_2[\delta(n - n_2) + \delta(n + n_2)]$$

$$= 0.2[\delta(n - 3) + \delta(n + 3)] + 0.1[\delta(n - 4) + \delta(n + 4)].$$

The response is as expected. Note that in addition to the added responses at values of n equal to $2n_1 = 6$; $2n_2 = 8$; $N - 2n_1 = 10$; $N - 2n_2 = 8$, there is also a response at $(n_1+n_2) = 7$. Again, this does not appear in our original analysis because of approximations. However, note that these additional terms are at least an order of magnitude less than the principal responses and they can be predicted.

Case 3: Two Reflections, Trapezoidal Shape Input Signal:

$x(n) = \{0.3, 0.7, 1, 1, 1, 0.6, 0.4, 0.2, 0, 0, ..0\}$ $n = 0,1,2, \ldots 15.$

(Fig. 16)

$h(n) = \varepsilon^{-0.25n}$ (Fig. 7)

$\alpha_1 = 0.2$; $\alpha_2 = 0.1$

$n_1 = 3$; $n_2 = 4$

This example has the same parameters as Case 2, but the function x(n) is different than Case 2. The plots of x(n), y(n), x(n)*h(n), y(n)*h(n), the cepstrum are shown in Figures 16-20. The results are the same as Case 2,

Case 4: One Reflection, Complex Reflection Coefficient

This example has the same parameters as Case 1 except for the reflection coefficient, α. For case 4,

$$\alpha = 0.2 + j0.2.$$

The plots of x(n), y(n), x(n)*h(n), y(n)*h(n), and the cepstrum are shown in Figures 21-25. The results are essentially the same as those of Case 1.

3.3 Summary

Cepstrum processing a signal as a time function has appeal in this detection problem because it requires the briefest time of observation. Although this technique worked well in the ideal computer simulation, there are several factors which may limit its usefulness in practice. Among these factors are:

1. The effect of vehicle orientation on accuracy of results.
2. The receiver transfer funtion. A careful study should be made

to insure that the receiver does not distort the original multipath relations.

3. Noise. The multipath transmission resulting from the obstacles will contribute low level signal particularly at the trailing edge of the main signal. These must not be masked by the noise.

4. Resolution and sampling rate. The sampling rate determines the minimum distance that two contiguous obstacles can be separated and still be resolved as two (not a single) obstacles.

Recall that the received signal when one reflection is present was represented as:

$$y(t) = x(t) + \alpha x(t - \tau) \tag{1}$$

and

$$d = c\tau. \tag{2}$$

The distance between the transmitting antenna and the source of the reflection is d and c is the free-space velocity of light and equals $300(10)^6$ meters/second.

If y(t) is sampled uniformly every T_s seconds,

$$y(mT_s) = x(mT_s) + \alpha x(mT_s - \tau) \tag{17}$$

or

$$y(n) = x(n) + \alpha x(n - \tau) \tag{18}$$

where $$n = mT_s. \tag{19}$$

Therefore: $$n(K+1) - n(K) = (m+1)T_s - mT_s = T_s. \tag{20}$$

Consequently, the shortest distance that can be resolved is:

$$d_{min} = cT_s = 300(10)^6\ T_s \text{ meters.} \tag{21}$$

In practice, various locations of obstacles probably will not correspond exactly to a sampling time n_i. Such an obstacle gives a cepstrum response corresponding to sampling times on either side of the time corresponding to its exact location. This will be demonstrated and discussed in the next section. If there are two or more obstacles in a distance corresponding to one sampling interval, T_s, they cannot be resolved. Equation 21 indicates that if T_s equals 10/3 nanoseconds, the resolution distance is 1 meter; however, if T_s equals 1 microsecond, the resolution distance is 300 meters.

5. There are other considerations common to all the methods considered in this detection problem which are discussed in the conclusions.

4. ANTENNA RADIATION PATTERN PROCESSING

4.1 Introduction

The radiation pattern of an antenna mounted on an aircraft or missile is composed of the radiation from the antenna itself plus the scattered fields from obstacles. If the contributions to the radiation pattern from components added to the vehicle which act as scatterers or obstacles can be identified, the information can be used to estimate the vehicle configuration. A technique which accomplishes this is described below.

Figure 4 represents an omnidirectional antenna at the origin plus N obstacles contributing to a far-field pattern, $E(\phi)$:

$$E(\phi) = 1 + \sum_{i=1}^{N} A_i \varepsilon^{j\gamma_i} \varepsilon^{j(2\pi/\lambda)d_i \cos\phi} \qquad (22)$$

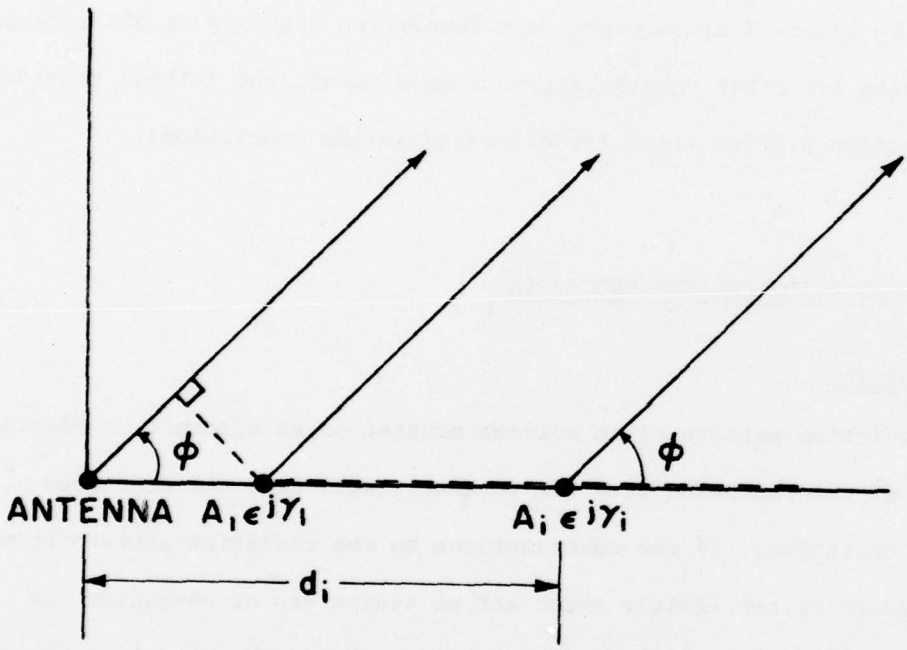

REFLECTIONS FROM OBSTACLES WHICH CONTRIBUTE TO ANTENNA FAR-FIELD

FIGURE 4

where:

A_i = amplitude of scattering signals,

γ_i = phase of scattering signals,

λ = wavelength of transmitted signal.

The field strength of the antenna at the origin has been assumed to equal 1.

Note that the scattering from the obstacles has been assumed omnidirectional also. This may not be true. However, as will be seen in Section 4, the sampling of the antenna pattern is done over a limited range of angle (never greater than $\pi/2$). Consequently, the hypothesis of omnidirectional scattering is reasonable.

To illustrate the method, assume that there is only one obstacle or scatterer a distance d from the antenna and that d/λ is an integer. These restrictions will be removed later. Under these conditions, the far field may be represented as:

$$E(\phi) = 1 + A\varepsilon^{j\gamma}\varepsilon^{+j((2\pi/\lambda)d\cos\phi)}. \tag{23}$$

Our problem is to determine d. We proceed as follows. The pattern is sampled at K values of ϕ. The method of determining ϕ_K, the K values of ϕ, results from the analysis below.

$$E(K) = E(\phi_K) = 1 + A\varepsilon^{j\gamma}\varepsilon^{+j(2\pi d/\lambda)\cos\phi_K} \tag{24}$$

Now take the discrete Fourier transform (DFT) of (24)

$$e(n) = \sum_{K=0}^{(N-1)} (1 + A\varepsilon^{j\gamma}\varepsilon^{+j((2\pi d/\lambda)\cos\phi_K)})\varepsilon^{-j(2\pi/N)nK} \tag{25}$$

$$= N\delta(n) + A\varepsilon^{j\gamma} \sum_{K=0}^{(N-1)} e^{-j\frac{2\pi}{N}K(n-(N/K)(d/\lambda)\cos\phi_K)} \quad ; \quad n = 0,1,2,\ldots(N-1) \tag{26}$$

If the sampling is done such that $\frac{N}{K}\frac{d}{\gamma}\cos\phi_K = n_0$, where n_0 is an integer constant, $1 \leq n_0 \leq (N-1)$,

$$e(n) = A\varepsilon^{j\gamma}\sum_{K=0}^{(N-1)}\varepsilon^{-j\frac{2\pi}{N}K(n-n_0)} + N\delta(n)$$

$$= NA\varepsilon^{j\gamma}\delta(n - n_0) + N\delta(n) \tag{27}$$

In other words, under these conditions the Fourier transform of the pattern yields an impulse at n_0.

How can this be used to determine d? This can be done choosing the ϕ_K's judiciously.

If we sample ϕ such that $\cos\phi = (\frac{K}{N})$, (28)*

$$\frac{d}{\lambda} = n_0. \tag{29}$$

This represents the essence of the method. To summarize, if the pattern is sampled in the non-uniform manner as described by (28), the DFT of this data includes an impulse at n_0 where $d = \lambda n_0$. Consequently, the position of the added obstacle with respect to the antenna has been estimated.

It has been assumed for simplicity that d/λ is an integer and that only one obstacle is present. These requirements are relaxed in the more general results developed below. Also, the validity of this method is demonstrated by the results of a number of computer simulations.

In the simulation program, the inverse FFT is used instead of the FFT and, therefore, the factor N multiplying (27) does not appear in the simulation results. Also, the magnitude only of the data multiplied by the scale

*This implies that the pattern is sampled over the range: $0 \leq \phi < \frac{\pi}{2}$.

factor 10 is plotted in all graphs.

Also, it should be pointed out that while this method resulted from a study of cepstrum techniques, it does not make use of cepstrum analysis. It is based on the following observations:

1. In (26), which is DFT of the sampled values of the radiation pattern,

$$\sum_{K=0}^{(N-1)} \varepsilon^{-j \frac{2\pi}{N} K(n-n_0)} \equiv 0$$

unless $(n-n_0) = 0$, where $n_0 = \frac{N}{K} \frac{d}{\lambda} \cos \phi_K$.

2. Consequently, if the sampling points, ϕ_K are picked such that $\cos \phi_K = K/N$, (26) will be zero for all n except the impulse at the origin and value at $n = n_0 = d/\lambda$. This is indicated in (27).

4.2 Simulation: d/λ = Integer; Single Reflection.

The computer program, NYAKA/CEPMLD, was used to carry out the simulation of this technique. A copy of the computer program is included in the appendix.

Case 1: Single Reflection

Figure 26: $A\varepsilon^{j\gamma} = 0.2$

$d/\lambda = 3$

Number of Sample Points = 8

Figure 27: $A\varepsilon^{j\gamma} = 0.2$

$d/\lambda = 3$

Number of Sample Points = 16.

Figure 28: $A\varepsilon^{j\gamma} = 0.2$

$d/\lambda = 3$

Number of Sample Points = 32

These three cases were run to indicate that the number of sample points does not affect the results.

Case 2. d_i/λ = Integer ; Multiple Reflections

Where more than one reflection is present and all are integer multiple of λ from the antenna at the origin, the analysis can be extended in an obvious manner. The DFT of (22) is:

$$e(n) = N[\delta(n) + \sum_{i=1}^{N} A_i \varepsilon^{j\gamma_i} \delta(n - n_N)] \qquad (30)$$

where $\cos \phi_K = \frac{K}{N}$ and $d_i = n_i\lambda$. This is illustrated in the following figures:

Figure 29: $A\varepsilon^{j\lambda} = 0.3$

$d/\lambda = 7$

Number of Sample Points = 32

Figure 30; $A_1\varepsilon^{j\gamma_1} = 0.2$; $A_2\varepsilon^{j\gamma_2} = 0.1$

$d_1/\lambda = 3$; $d_2/\lambda = 6$

Number of Sample Points = 32.

Figure 31: $A_1\varepsilon^{j\gamma_1} = 0.4$; $A_2\varepsilon^{j\gamma_2} = 0.1$; $A_3\varepsilon^{j\gamma_3} = 0.2$

$d_1/\lambda = 2$; $d_2/\lambda = 7$; $d_3/\lambda = 13$

Number of Sample Points = 32.

These results are as predicted by the analysis.

Case 3: d/λ = Noninteger; Integer Program

In this series of simulations the same processing (or program) was used as in cases 1 and 2, but d was not equal to integer multiples of λ. Notice that it is still possible to estimate the locations of the sources of reflection. Experience can improve the accuracy of these estimates. Better estimates can be obtained by more sophisticated processing such as described in Cases 4 and 5.

Fig. 32: $A\varepsilon^{j\gamma} = 0.2$

$d/\lambda = 3.2$

Fig. 33: $A\varepsilon^{j\gamma} = 0.2$

$d/\lambda = 3.5$

Fig. 34: $A\varepsilon^{j\gamma} = 0.2$

$d/\lambda = 3.8$

Fig. 35: $A_1\varepsilon^{j\gamma_1} = 0.2$; $A_2\varepsilon^{j\gamma_2} = 0.2$; $A_3\varepsilon^{j\gamma_3} = 0.4$

$d_1/\lambda = 2.25$; $d_2/\lambda = 2.75$; $d_3/\lambda = 5$

Fig. 36: $A_1\varepsilon^{j\gamma_1} = 0.3$; $A_2\varepsilon^{j\gamma_2} = 0.1$; $A_3\varepsilon^{j\gamma_3} = 0.2$

$d_1/\lambda = 2.3$; $d_2/\lambda = 2.65$; $d_3/\lambda = 5$

Observe that in all these cases, the largest response occurs at the value of n that corresponds to the best approximation of d/λ. However, experience and/or further analysis is required to develop rules about whether the spurious responses correspond to weak reflections or may be disregarded. For instance in Figure 33 where $d/\lambda = 3.5$, the response is

symmetrical about that point and, with experience, one would interpret this as a single reflection at $d/\lambda = 3.5$.

Because, in general, d/λ will not equal an integer, methods of detecting any value of d were investigated. Some of these results are described below.

Case 4: d/λ = Noninteger; Modified Processing; One Reflection

In the analysis of this method in Section 4.1 in equation 25, we set

$$\frac{N}{K}\frac{d}{\lambda}\cos\phi_K = n_0 \tag{31}$$

and

$$\cos\phi_K = \frac{K}{N} \tag{32}$$

so that

$$\frac{d}{\lambda} = n_0$$

and a response occurred at n_0.

On the other hand, consider the case where:

$$\frac{d}{\lambda} = \left(m + \frac{p}{q}\right) \quad ; \quad p,q,m \text{ are integers} \tag{33}$$

Also assume that: $N = Jq$; J and q are integers (34)

Now, for a response at n_0,

$$n_0 = \frac{N}{K}\frac{d}{\lambda}\cos\phi = Jq\,\frac{(qm + p)}{qK}\cos\phi_K \tag{35}$$

$$\text{Let } \cos\phi_K = \frac{r_0 K}{J(qm + p)} \quad ; \quad K = 0,1,2 \ldots (N-1) \tag{36}$$

and $n_0 = r_0$.

Because $|\cos\phi_K| \leq 1$ and $0 \leq K \leq (N-1)$,

$$r_0 \leq \frac{J(qm + p)}{(N - 1)} \quad . \tag{37}$$

Equation (36) gives the rule for determining the sample values of ϕ_K. Under these conditions, a response at $n = r_0$ indicates an obstacle at $d/\lambda = (m + \frac{p}{q})$. This is illustrated in Figures 37 and 38.

Fig. 37: $A\varepsilon^{j\gamma} = 0.45$

$$\frac{d}{\lambda} = 3.5 = 3 + \frac{1}{2}$$

$$\text{Cos } \phi_K = \frac{1K}{16(7)} = \frac{K}{112} \quad ; \quad K = 0,1,2 \ldots (N-1).^*$$

A response, $\delta(n - 1) = 0.45$, is observed in Fig. 37.

Fig. 38: $A\varepsilon^{j\gamma} = 0.45$

$$\frac{d}{\lambda} = 10.5 = 3(3.5) = 3(3 + \frac{1}{2})$$

$$\cos \phi_K = \frac{K}{112} \quad ; \quad K = 0,1,2,\ldots (N-1)$$

In this case where $d/\lambda = 3(m + \frac{p}{q})$, the response occurs at n=3 as indicated in Fig. 38.

Case 5: d/λ = Noninteger; Modified Processing; Multiple Reflections

Routines were developed to detect multiple reflections located st noninteger values of d/λ. One will be illustrated for a particular case of two reflections. Rewrite (24), the equation for the sampled field, as:

$$E(K) = E(\phi_K) = 1 + A_1\varepsilon^{j\gamma_1}\varepsilon^{j(\frac{2\pi}{\lambda}d_1\cos\phi_K)} + A_2\varepsilon^{j\gamma_2}\varepsilon^{j(\frac{2\pi}{\lambda}d_2\cos\phi_K)}$$

*In the processing modified for noninteger values of d/λ, ϕ is sampled over an even smaller range than $\pi/2$.

$$e(n) = \sum_{K=0}^{(N-1)} [1 + A_1 \varepsilon^{j\gamma_1} \varepsilon^{j\frac{2\pi}{\lambda} d_1 \cos\phi_K} + A_2 \varepsilon^{j\gamma_2} \varepsilon^{j\frac{2\pi}{\lambda} d_2 \cos\phi_K}] \varepsilon^{-j\frac{2\pi}{N} nK}$$

$$= N\delta(n) + \sum_{K=1}^{(N-1)} [A_1 \varepsilon^{j\gamma_1} \varepsilon^{-j(n - \frac{d_1}{\lambda} \frac{N}{K} \cos\phi_K)}$$

$$+ A_2 \varepsilon^{j\gamma_2} \varepsilon^{-j(n - \frac{d_2}{\lambda} \frac{N}{K} \cos\phi_K)}] \varepsilon^{-j\frac{2\pi}{N} K}$$

We wish to choose the sample points, ϕ_K, of the antenna pattern such that:

$$n_1 - \frac{d_1}{\lambda} \frac{N}{K} \cos \phi_K = 0 = n_2 - \frac{d_2}{\lambda} \frac{N}{K} \cos \phi_K.$$

Under this condition, a response at n_1 will indicate a source of reflection at d_1 and a response at n_2 will indicate a source of reflection at d_2.

Let: $\frac{d_1}{\lambda} = (m_1 + \frac{p_1}{q_1})$ and $\frac{d_2}{\lambda} = (m_2 + \frac{p_2}{q_2})$.

Then: $\cos \phi_K = n_1 \frac{K}{N} (\frac{q_1}{m_1 q_1 + p_1}) = n_2 \frac{K}{N} (\frac{q_2}{m_2 q_2 + p_2})$

Suppose: $N = 32$; $\frac{d_1}{\lambda} = 1.25 = \frac{5}{4}$; $\frac{d_2}{\lambda} = 2.5 = \frac{5}{2}$.

$$\cos \phi_K = n_1 K \frac{(4)}{32(5)} = n_2 K \frac{(2)}{32(5)}$$

$$= n_1 \frac{K}{40} = \frac{n_2 K}{2(40)}$$

Therefore, if we let $n_1 = 1$ and $n_2 = 2$,

$$\cos \phi_K = \frac{K}{40} \quad ; \quad K = 0,1,2,3, \ldots (N-1)$$

and the sample points are determined by the formula:

$$\phi_K = \arccos \frac{K}{40} \quad ; \quad K = 0, 1, 2, \ldots (N-1).$$

This is illustrated in Fig. 39.

$$A_1 \varepsilon^{j\gamma_1} = 0.3 \quad ; \quad A_2 \varepsilon^{j\gamma_2} = 0.45$$

$$\frac{d_1}{\lambda} = 1.25 \quad ; \quad \frac{d_2}{\lambda} = 2.5$$

$$\cos \phi_K = \frac{K}{40} \quad ; \quad K = 0, 1, 2, 3 \ldots (N-1)$$

The results are as predicted by the analysis.

4.3 Summary

The analysis and simulation in Section 4 demonstrate the soundness of technique of detecting multiple reflections of a vehicle by monitoring its RF transmissions. This was accomplished by a special non-uniform sampling of its radiation pattern and applying the FFT. Some of the unsolved problems are:

1. The analysis assumed a linear array of reflectors. This must be generalized to include the case of reflectors at arbitrary positions.

2. The problem of the minimum distance between two obstacles that can be resolved by this method has not been studied. It is clear that $d \geq \lambda$ can be resolved.

3. The effect of noise has not been considered.

4. General problems are included in the conclusions.

5. CONCLUSION

The theoretical soundness of applying cepstrum and associated techniques to the problem of determining a vehicle's configuration by monitoring its RF external transmissions has been demonstrated by the analysis and simulation developed in this report. The results are sufficiently promising to warrant further study to determine if these methods are practically feasible.

A number of assumptions and limitations in this study should be investigated.

1. It was assumed that the obstacles can be represented as point sources of reflections with omnidirectional scattering patterns. This must be checked.

2. Reflections and scattering from the terrain and other sources have been neglected. The validity of this assumption must be investigated.

3. Performance of this technique in a real, noisy environment must be investigated.

4. The ability of this technique to resolve distinct obstacles, in practice, must be verified. This is related to (1) above.

5. Throughout the work in this report we have solved for the distance, d, between an antenna and a scattering obstacle. This does not give a precise location of the obstacle. This result, d, depends on the difference in total time of transmission of the received signal from the antenna and the scattering obstacle. Therefore, the point determined by d can lie anywhere on an ellipse whose foci are the transmitting antenna

and the receiver. Strategies, such as performing more than one measurement, should be studied which will give a better estimate of the exact location of the source of reflection or scattering.

6. In addition, there should be further study of problems peculiar to the specific method of signal processing used as discussed in Section 3 and Section 4. This will help determine which specific method is best.

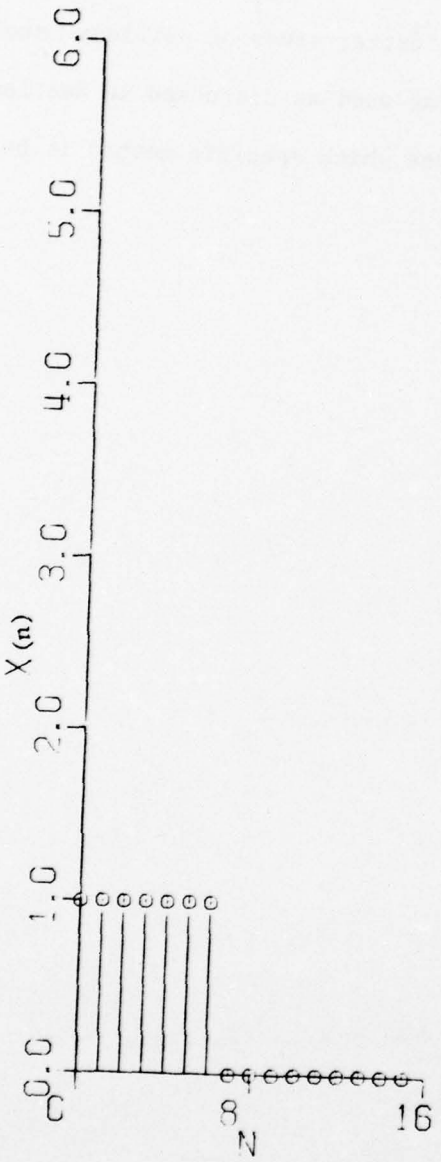

Fig. 5. x(n)

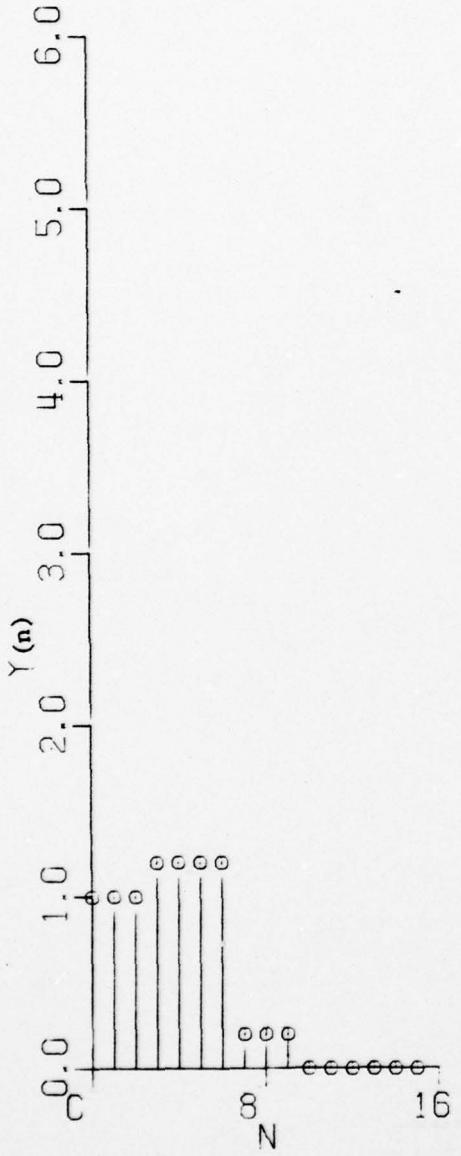

Fig. 6. $y(n) = x(n) + \alpha x(n-n_o) = x(n) + 0.2x(n-3)$

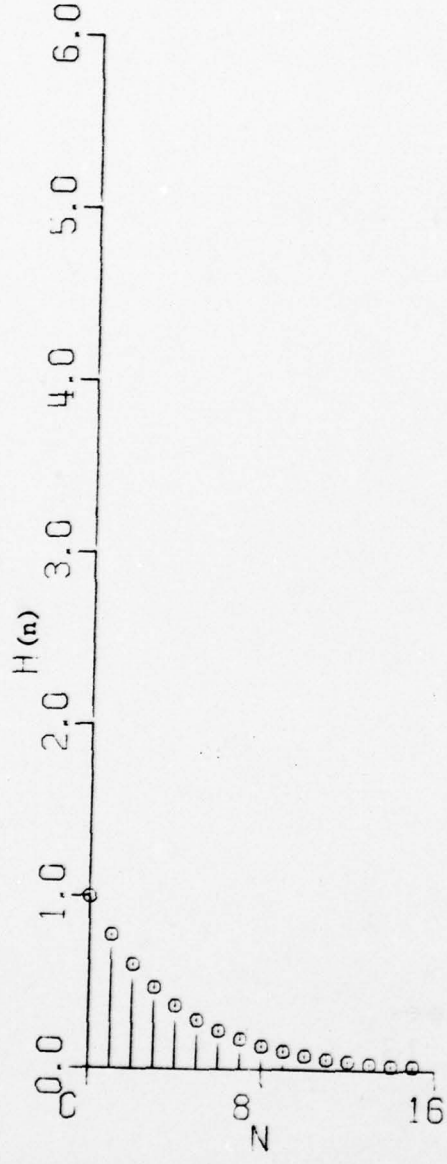

Fig. 7. $h(n) = E^{-0.25n}$

Fig. 8. 4[x(n)*h(n)] = 4R(n)

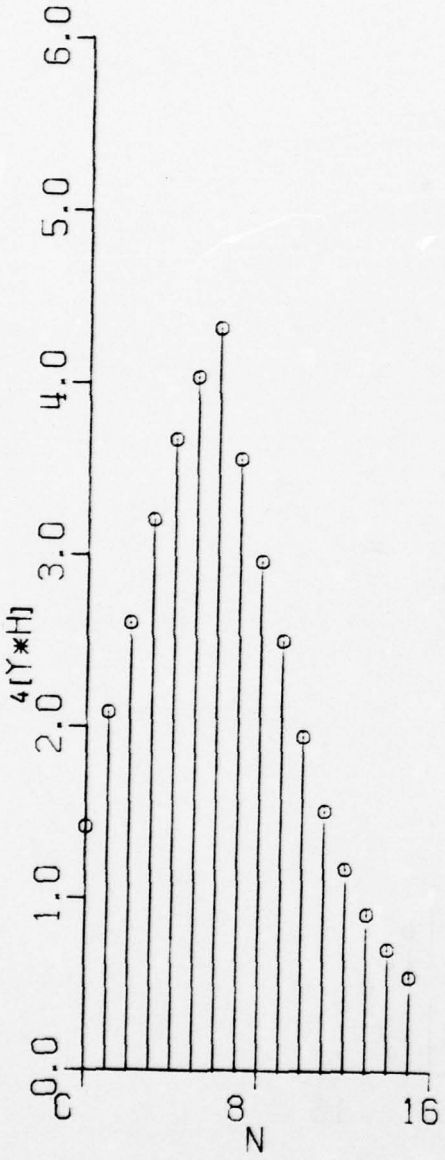

Fig. 9. 4[y(n)*h(n)] = 4s(n)

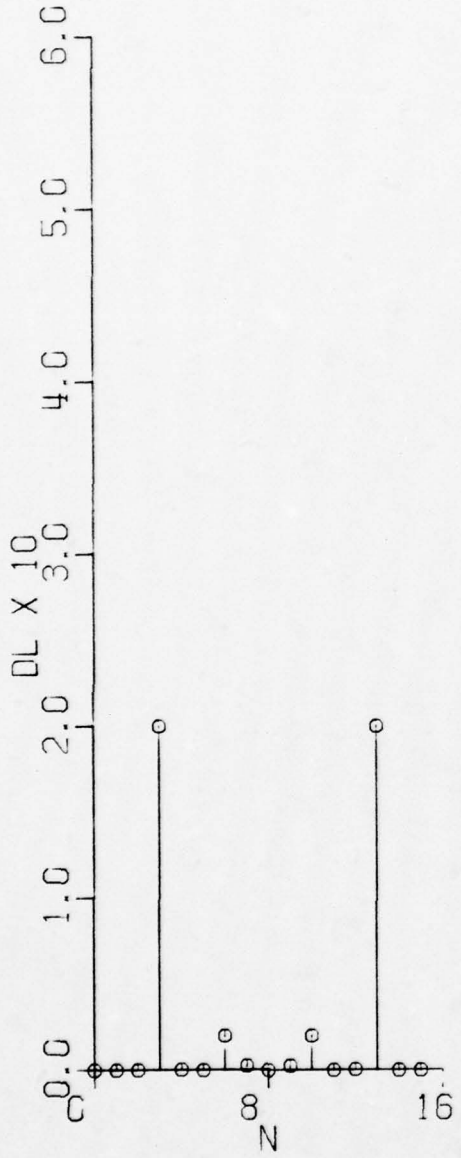

Fig. 10. Real Cepstrum of s(n) = h(n)*[x(n) + 0.2x(n-3)]
(see x(n) in Fig. 5; h(n) in Fig. 7)

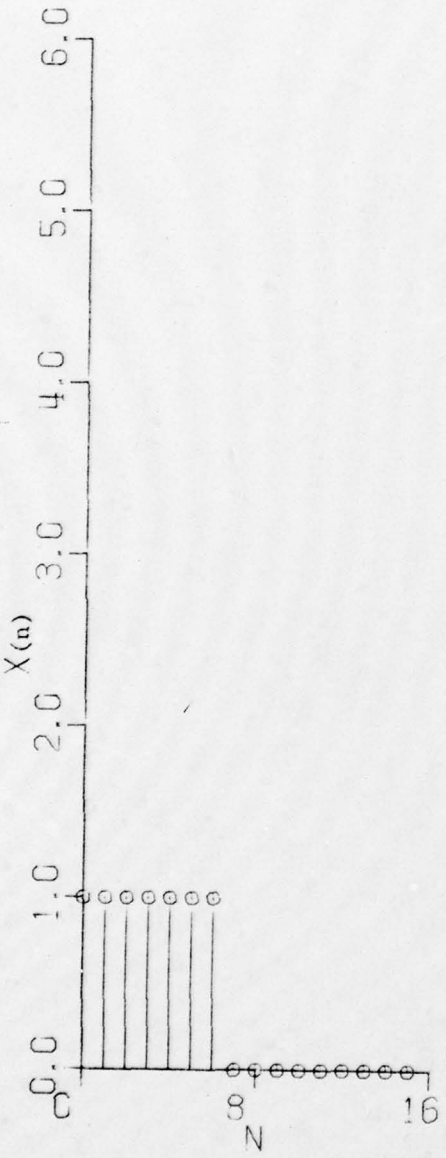

Fig. 11. x(n); 2 Reflections

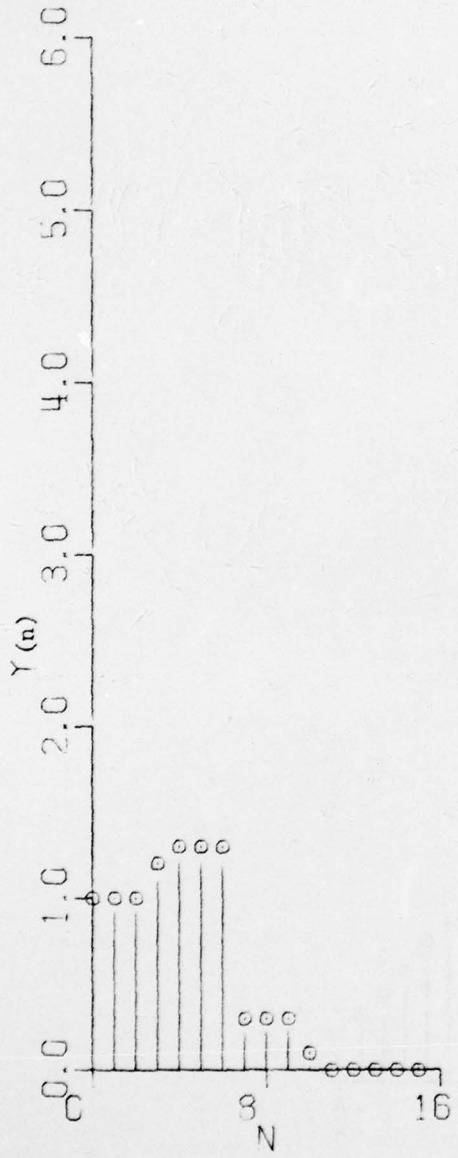

Fig. 12. $y(n) = x(n) + 0.2x(n-3) + 0.1x(n-4)$

Fig. 13. 4R(n) = 4[x(n)*h(n)]

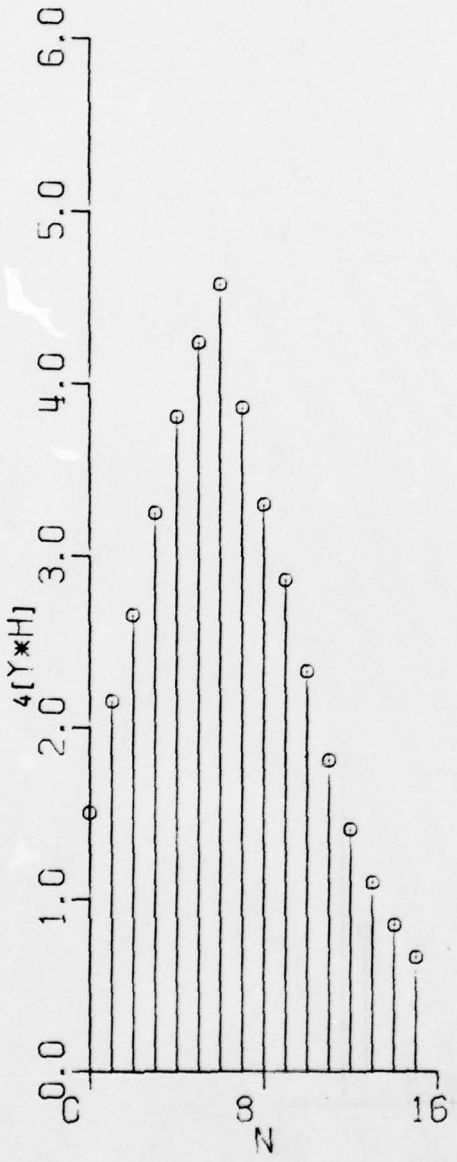

Fig. 14. 4s(n) = 4[y(n)*h(n)]

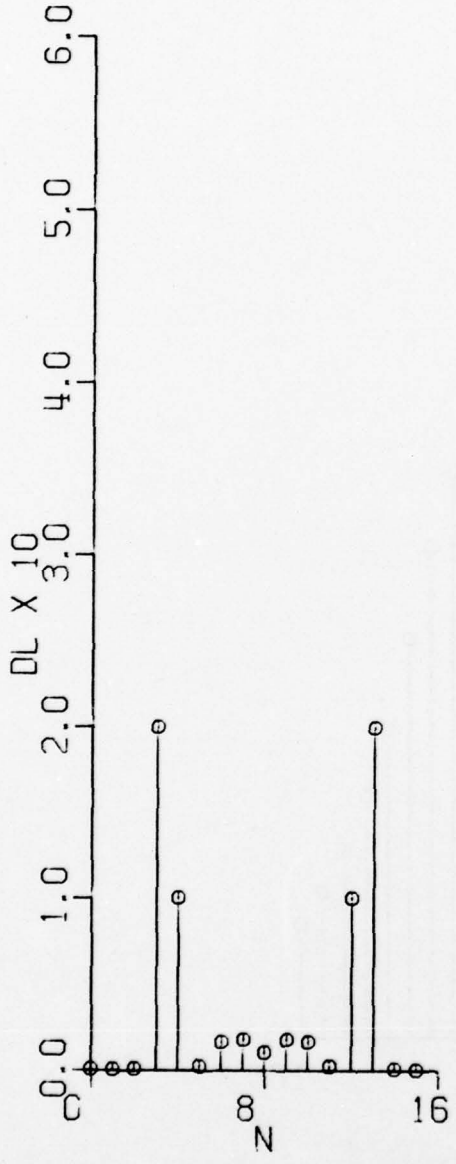

Fig. 15. Cepstrum of s(n) = h(n)*[x(n) + 0.2x(n-3) + 0.1x(n-4)] (See x(n) in Fig. 11; see h(n) in Fig. 7.)

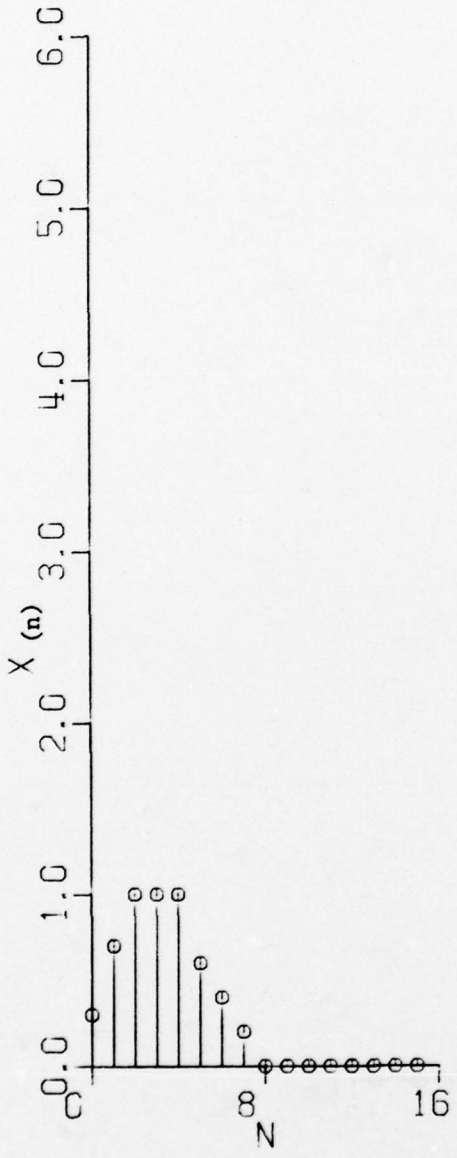

Fig. 16. x(n); Trapezoidal Wave Shape

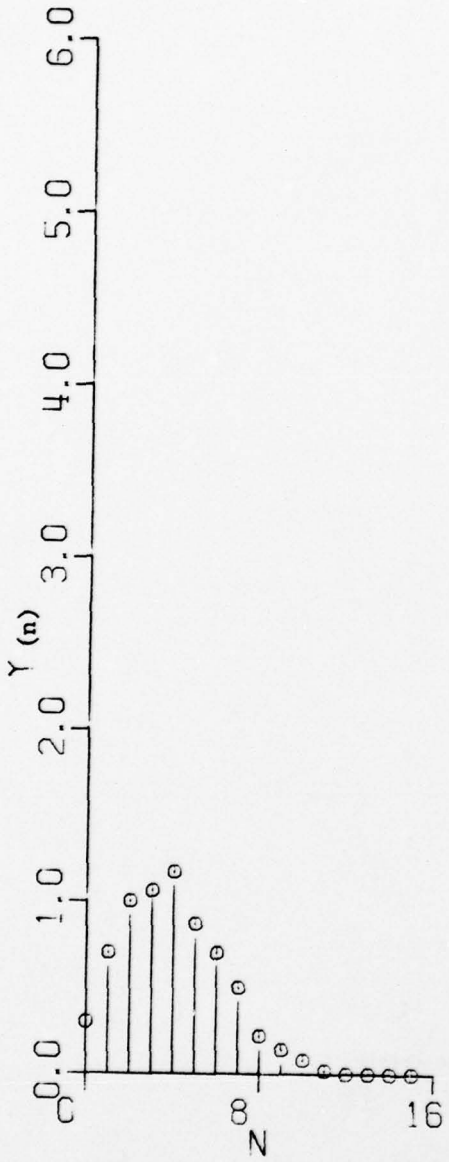

Fig. 17. y(n); Two Reflections; Trapezoidal Input

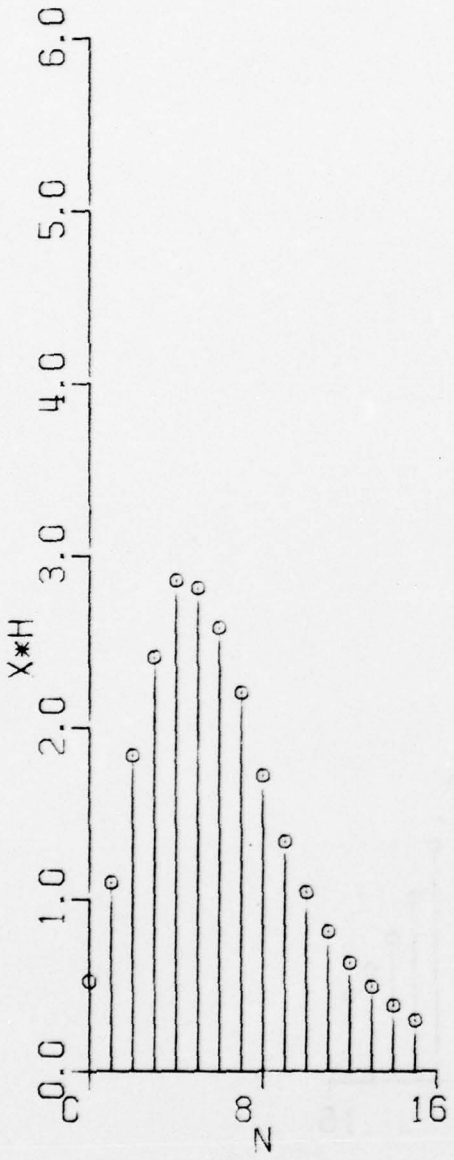

Fig. 18. 4R(n) = 4x(n)*h(n); Two Reflections; Trapezoidal Input

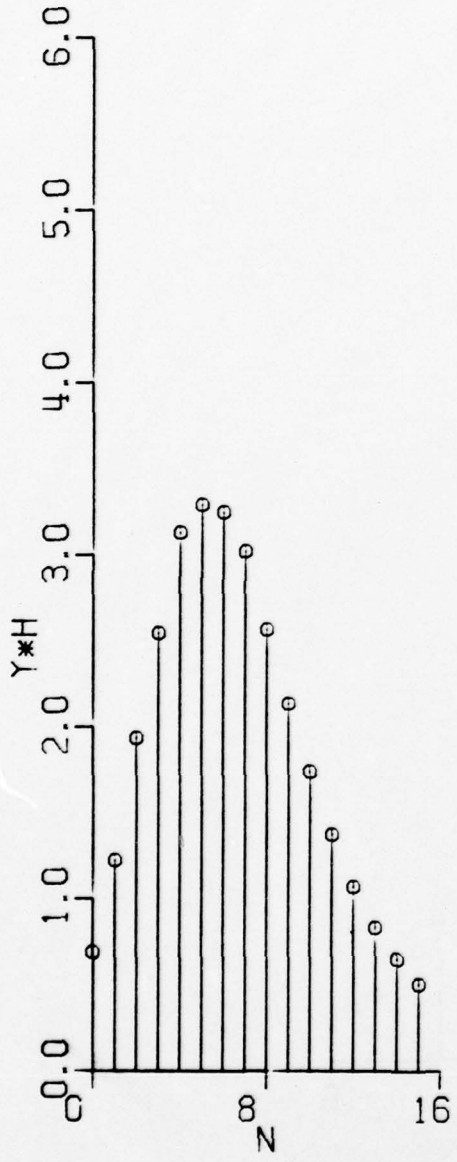

Fig. 19. 4s(n) = 4y(n)*h(n); Two Reflections; Trapezoidal Input

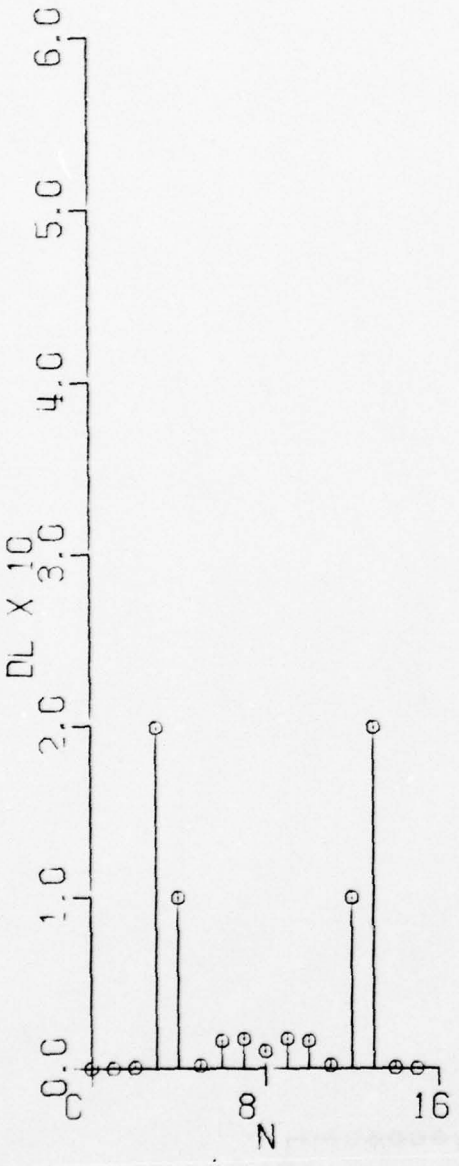

Fig. 20. Real Cepstrum of s(n) = h(n)*[x(n) + 0.2x(n-3) + 0.1x(n-4)]; Trapezoidal Input

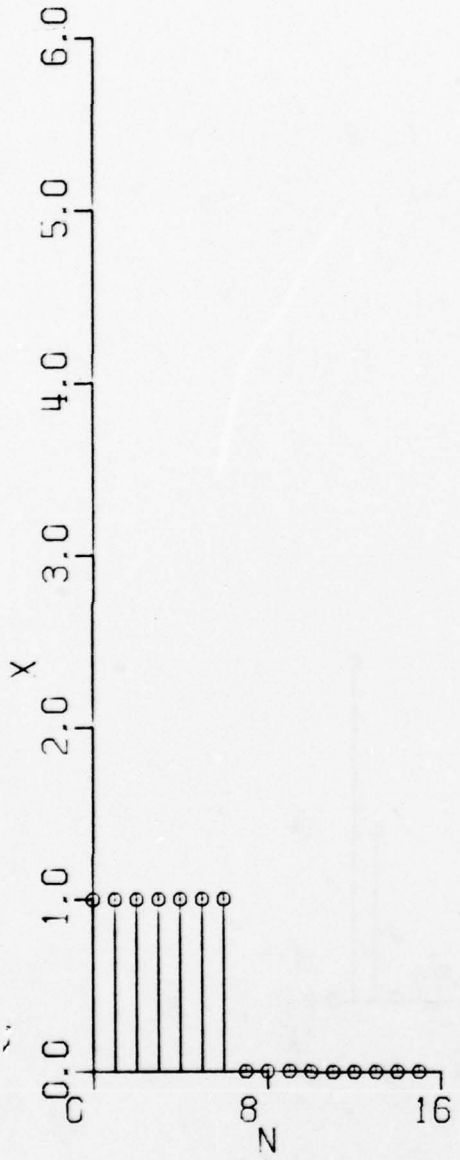

Fig. 21. x(n)

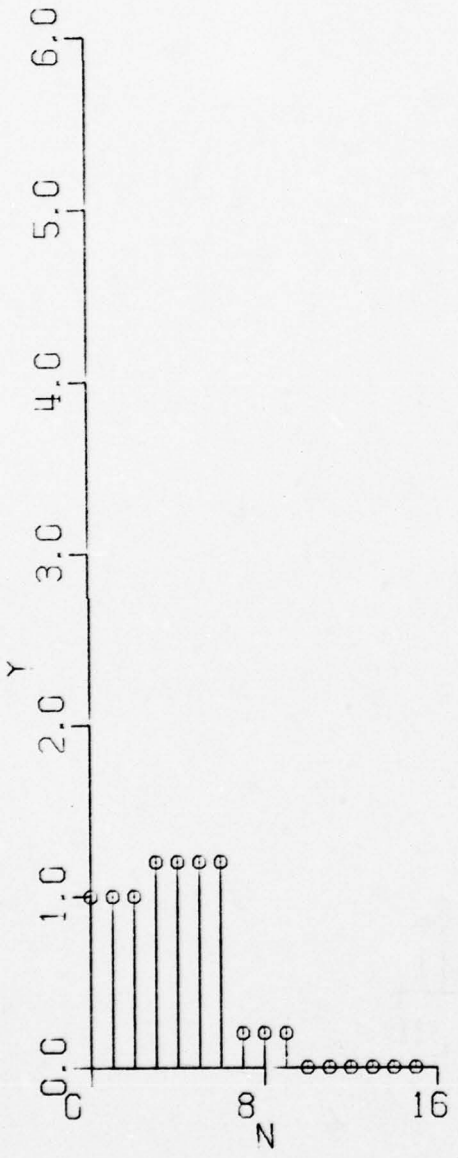

Fig. 22. y(n); One Reflection; Complex Reflection Coefficient

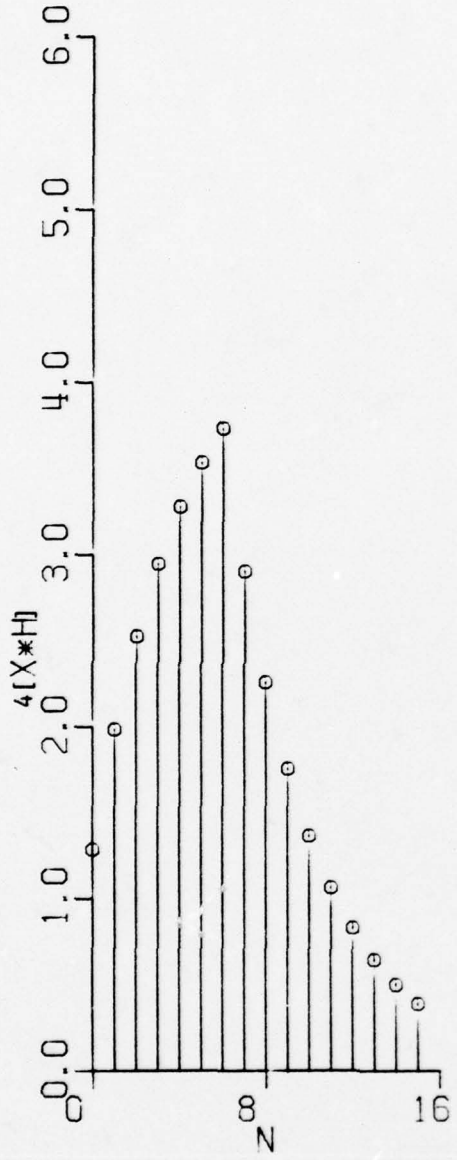

Fig. 23. 4R(n) = 4x(n)*h(n)

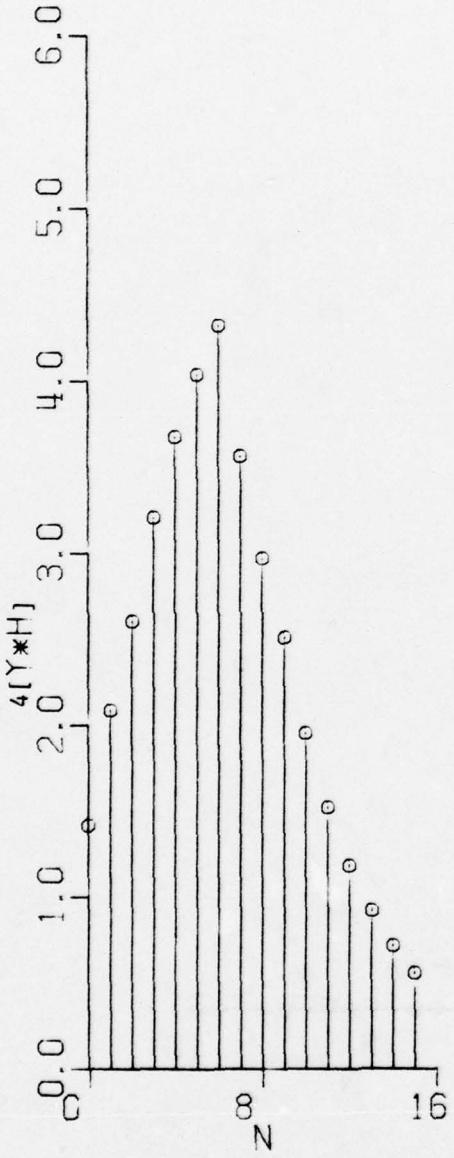

Fig. 24. 4s(n) = 4y(n)*h(n)

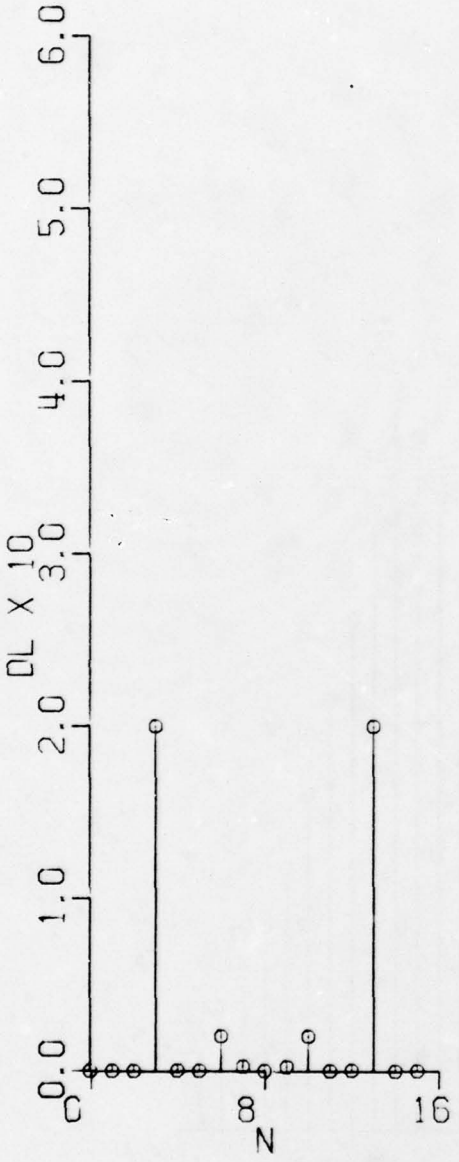

Fig. 25. Real Cepstrum of s(n) = [x(n) + (0.2 + j0.2)x(n-3)]

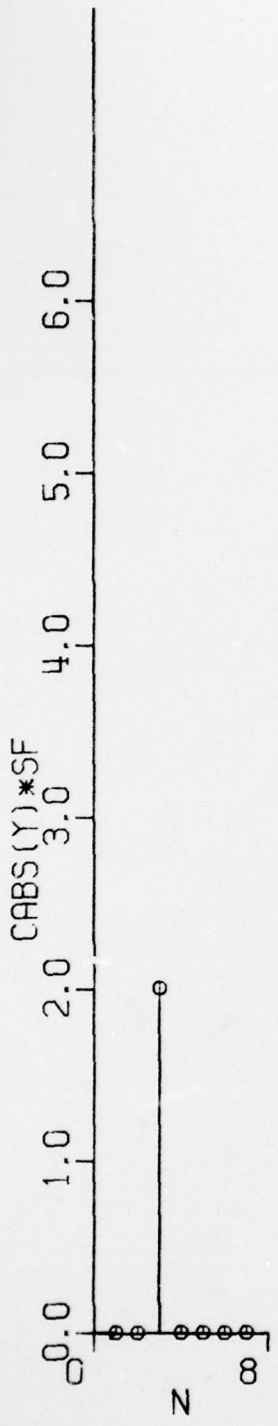

Fig. 26. Delay Determination: $E(\phi) = 1 + 0.2E^{j2\pi(3\cos\phi)}$
A = 0.2; $d/\lambda = 3$; N = 8; SF = 10

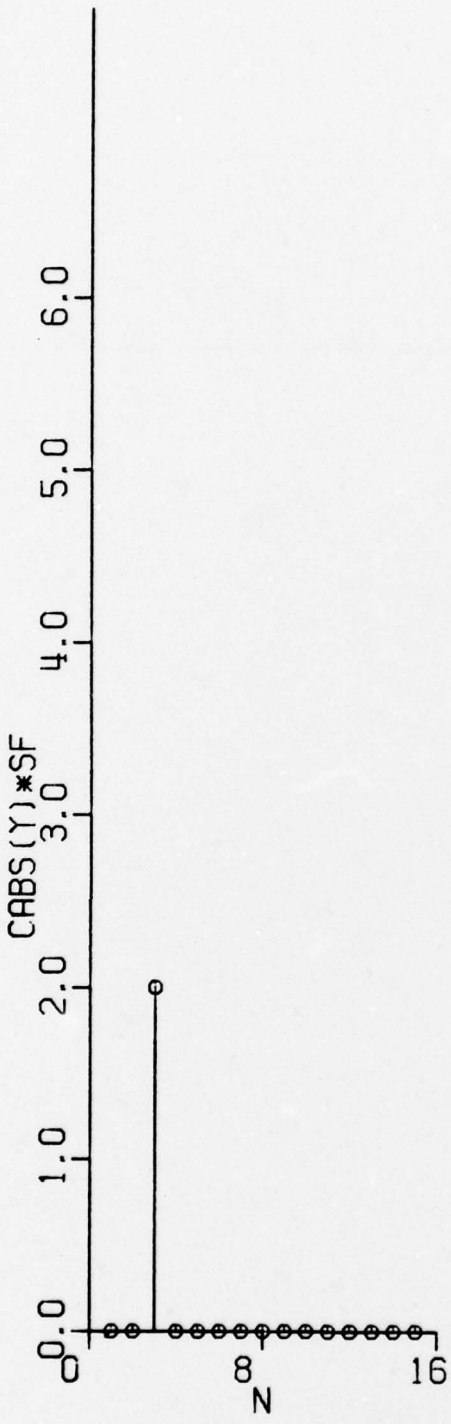

Fig. 27. Delay Determination: A = 0.2; d/λ = 3; N = 16; SF = 10

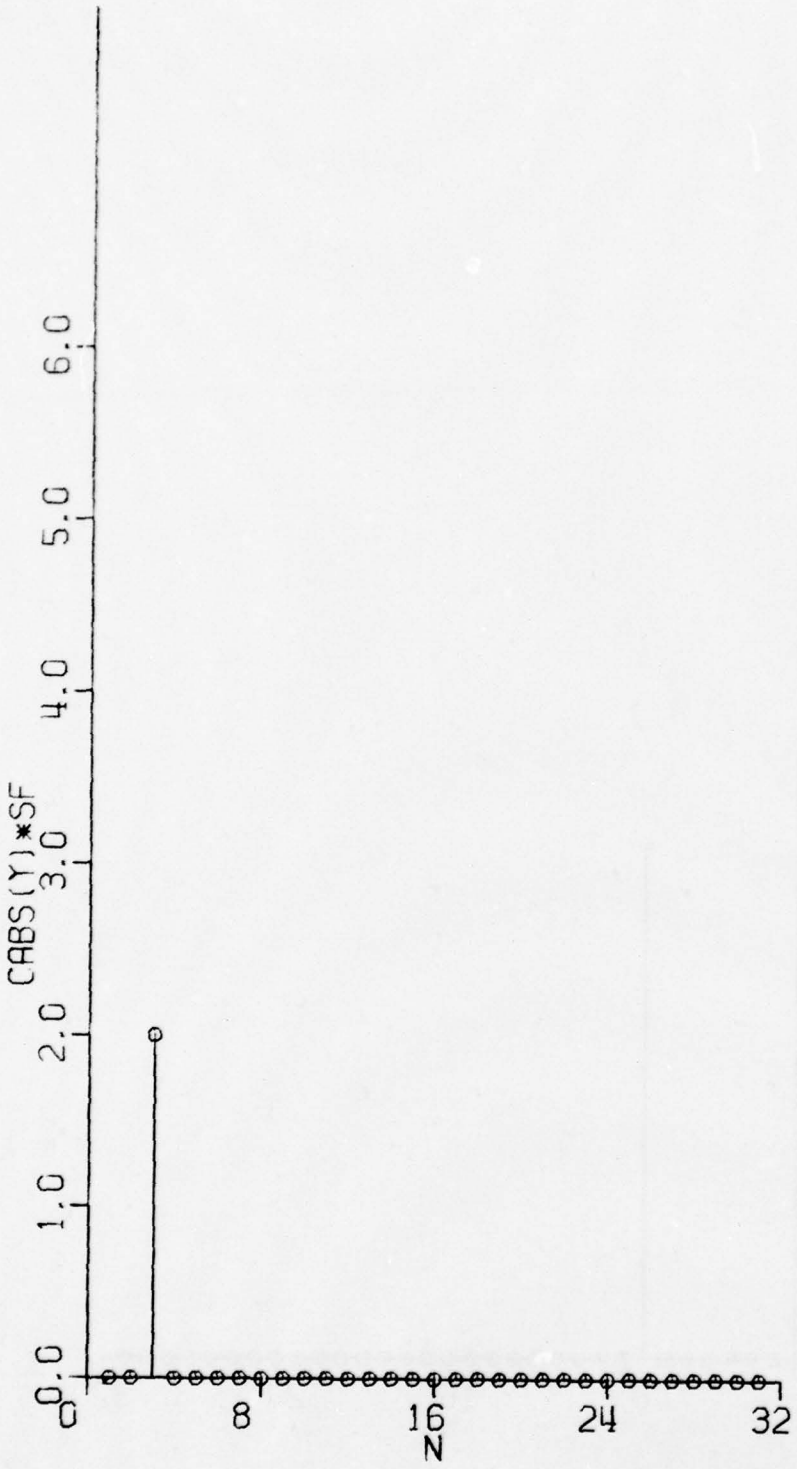

Fig. 28. Delay Determination: A = 0.2; d/λ = 3; N = 32; SF = 10

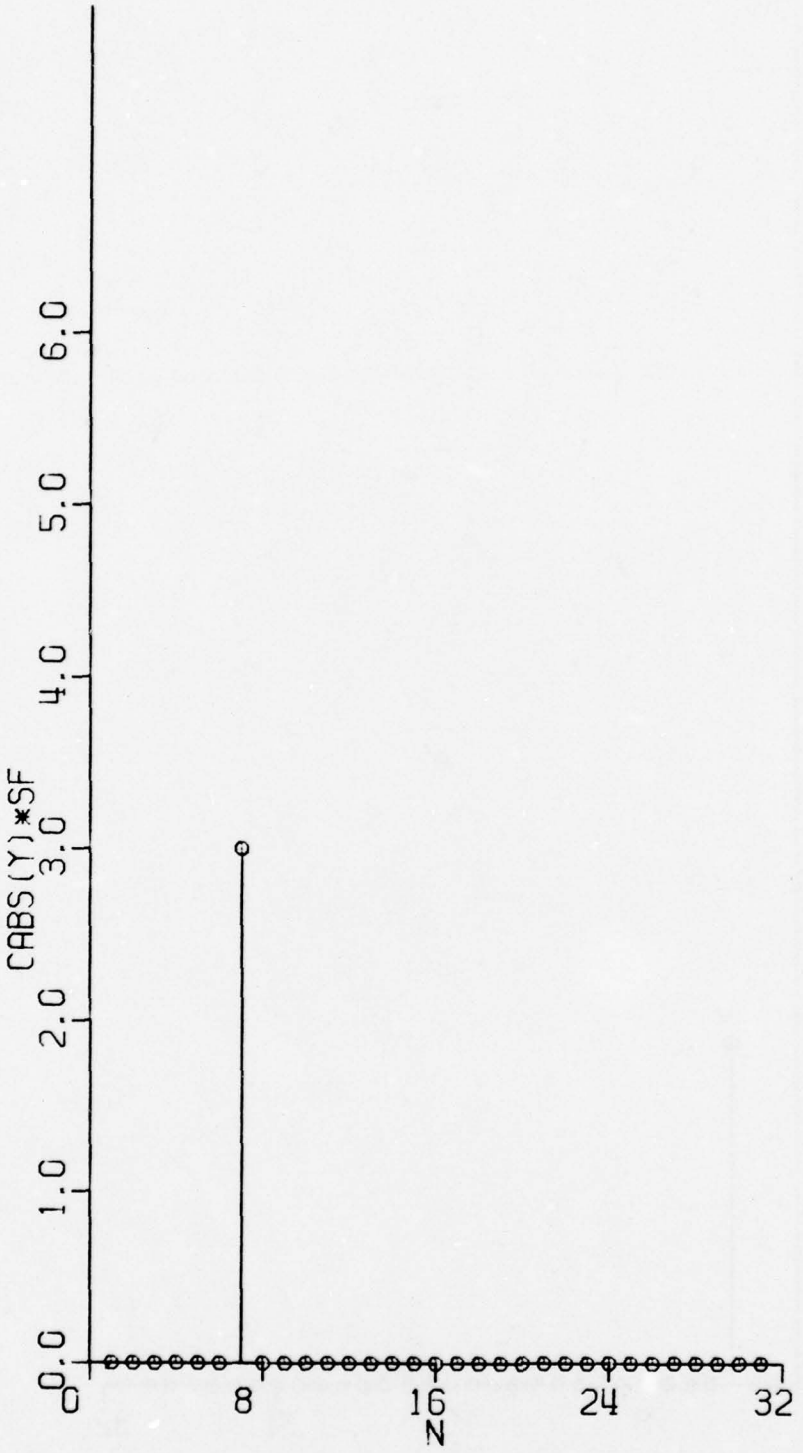

Fig. 29. Delay Determination: A = 0.3; d/λ = 7; N = 32; SF = 10

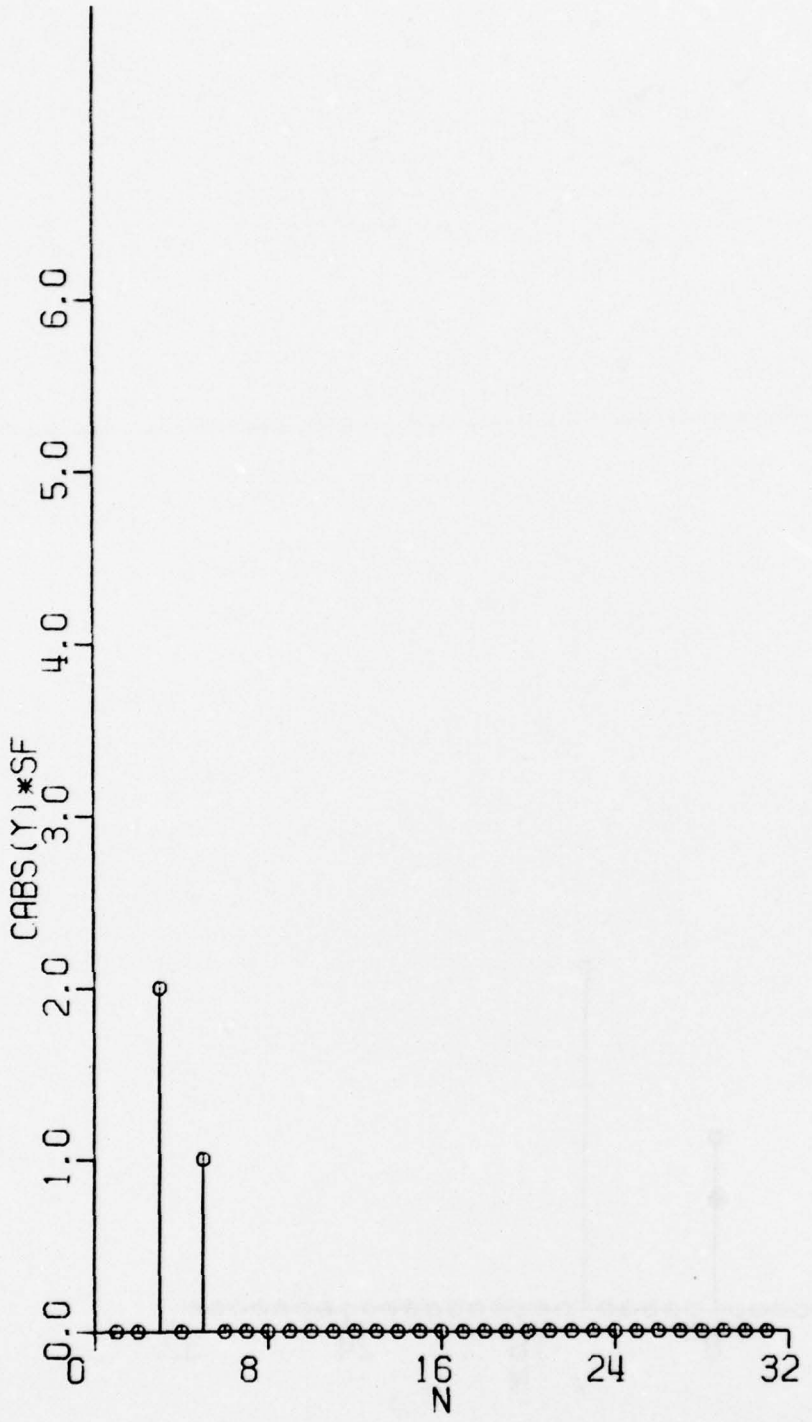

Fig. 30. Delay Determination: $A_1 = 0.2$; $d_1/\lambda = 3$; $A_2 = 0.1$; $d_2/\lambda = 6$; N = 32; SF = 10

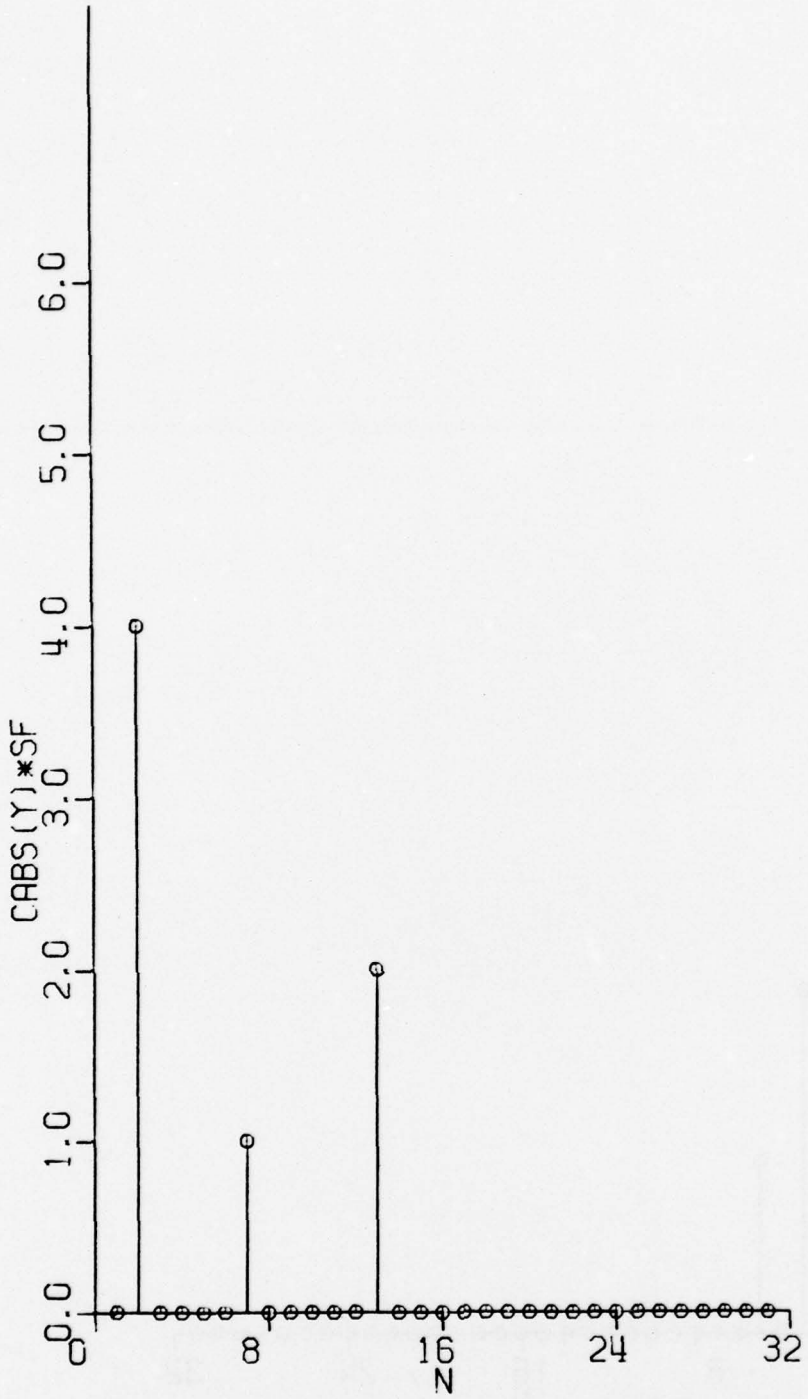

Fig. 31. Delay Determination: $A_1 = 0.4$; $d_1/\lambda = 2$; $A_2 = 0.1$; $d_2/\lambda = 7$; $A_3 = 0.2$; $d_3/\lambda = 13$; $N = 32$; $SF = 10$

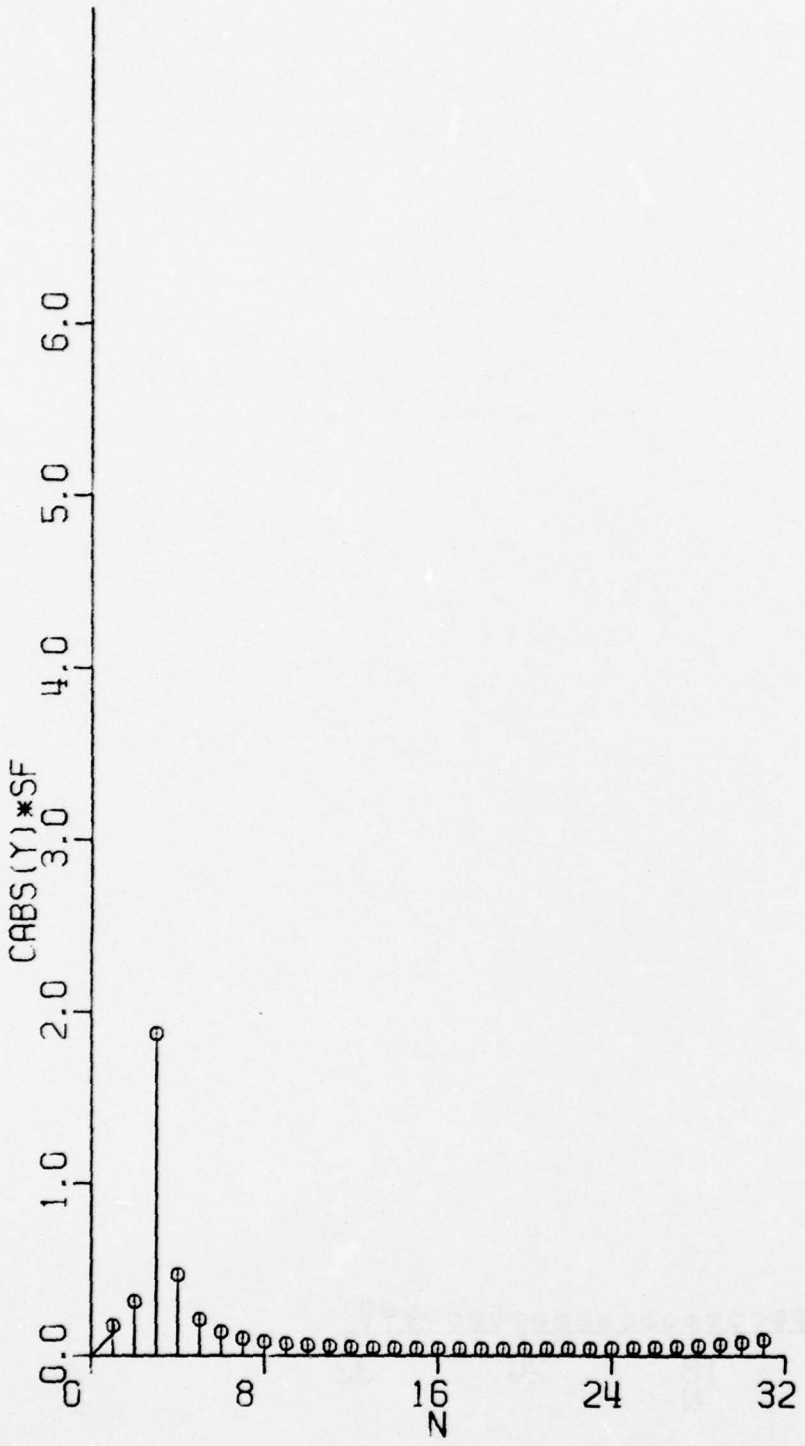

Fig. 32. Delay Determination: A = 0.2; d/λ = 3.2; N = 32; SF = 10

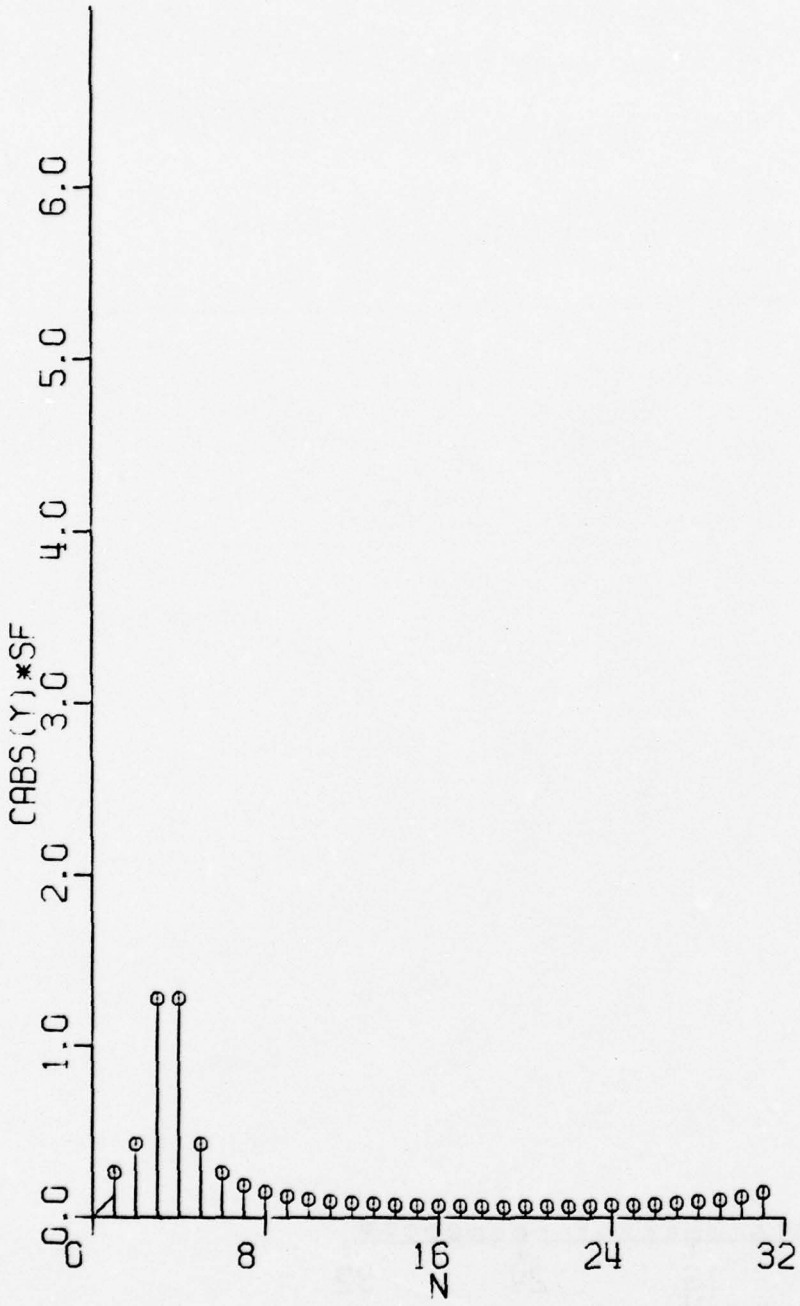

Fig. 33. Delay Determination: A = 0.2; d/λ = 3.5; N = 32; SF = 10

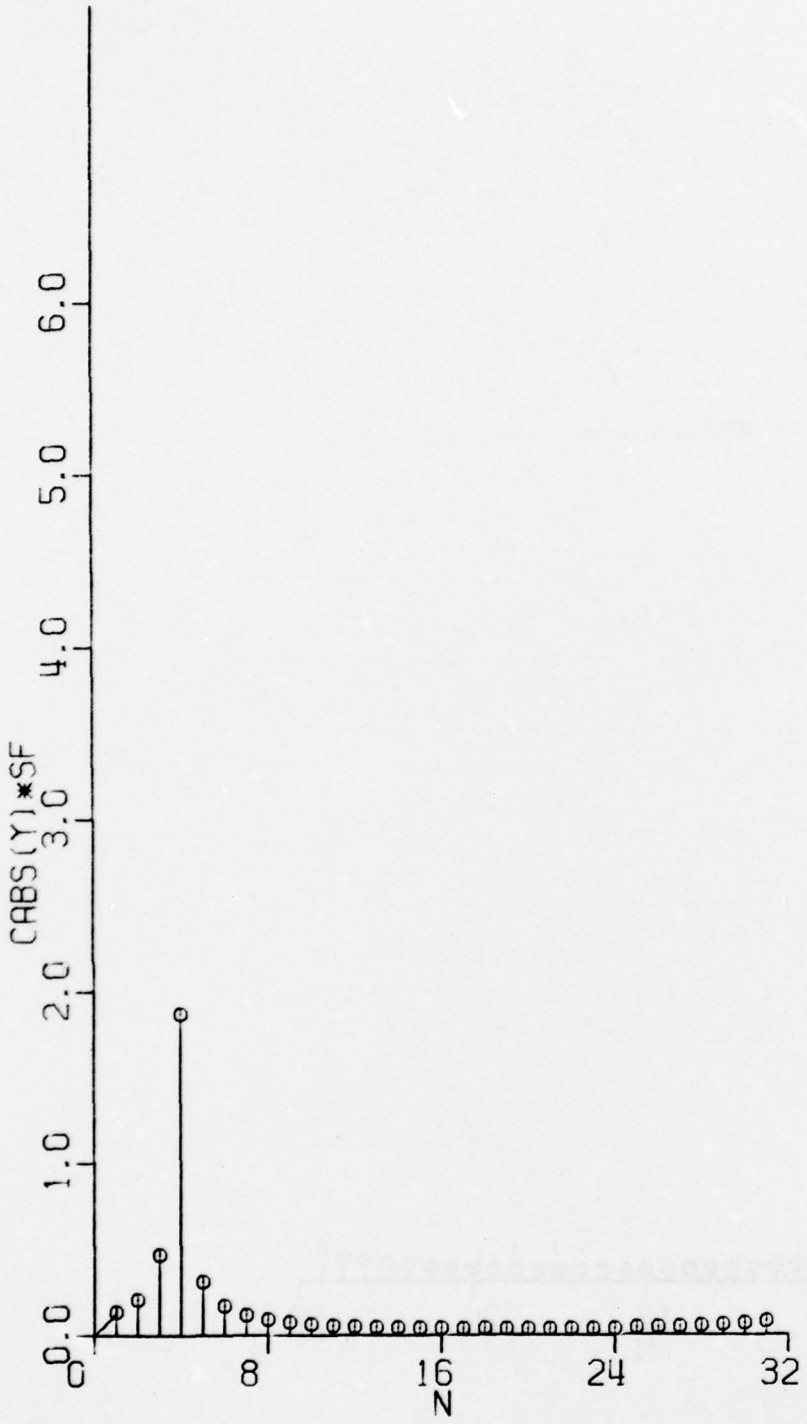

Fig. 34. Delay Determination: A = 0.2; d/λ = 3.8; N = 32; SF = 10

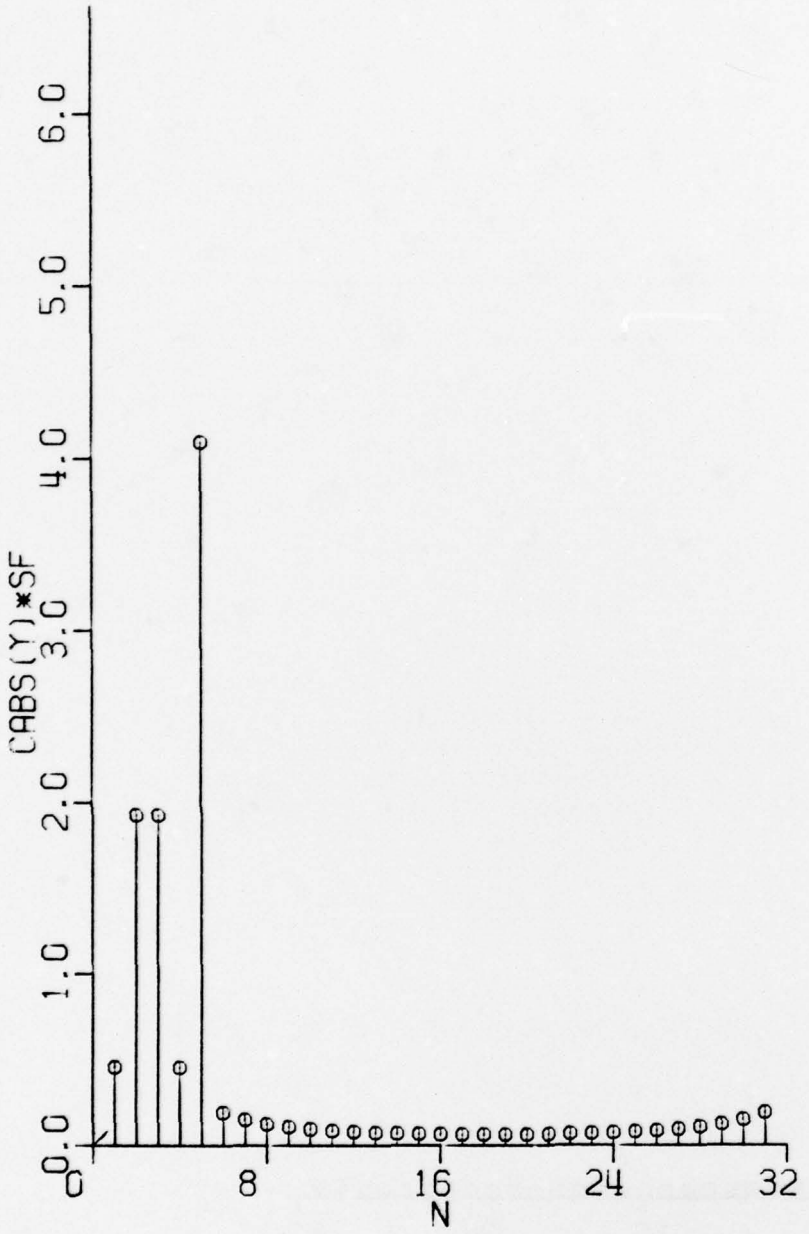

Fig. 35. Delay Determination: $A_1 = 0.2$; $d_1/\lambda = 2.25$; $A_2 = 0.2$; $d_2/\lambda = 2.75$; $A_3 = 0.4$; $d_3/\lambda = 5$; N = 32; SF = 10

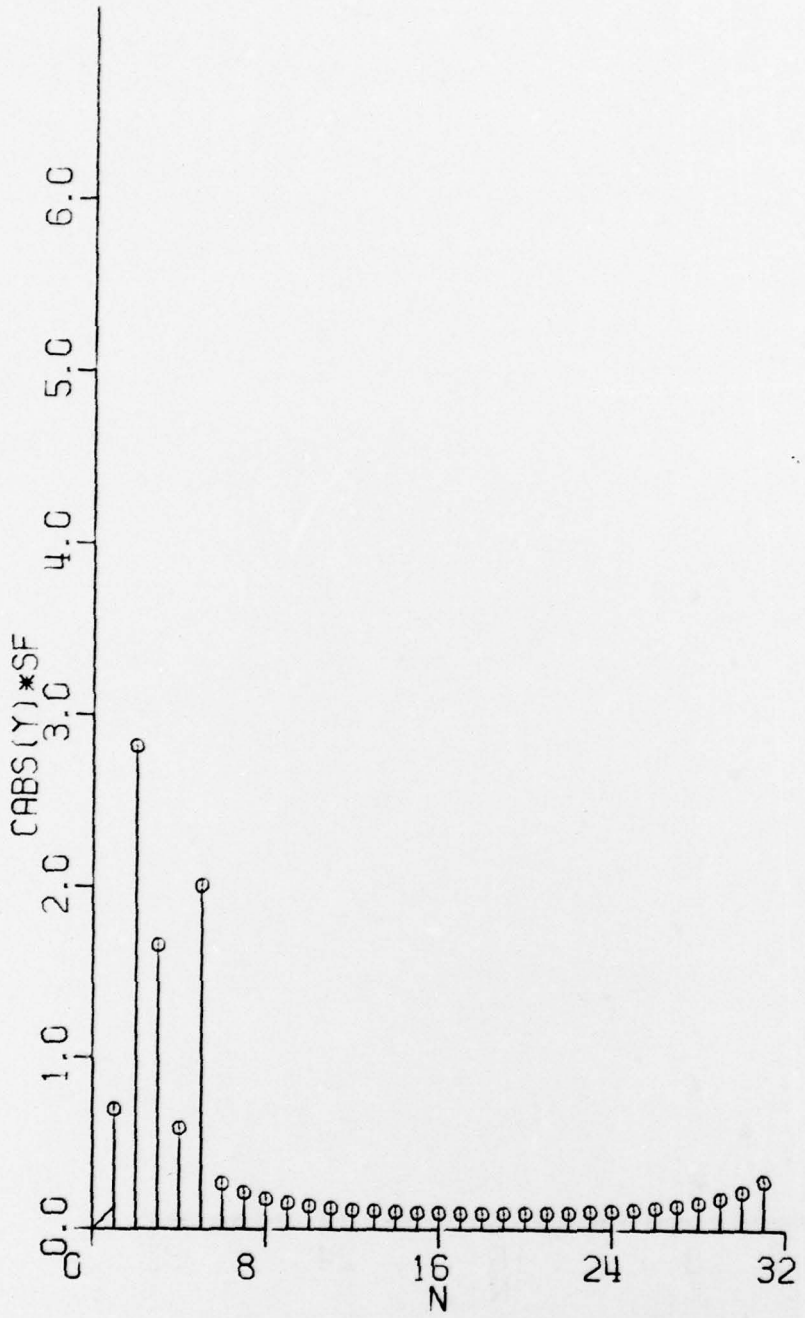

Fig. 36. Delay Determination: $A_1 = 0.3$; $d_1/\lambda = 2.3$; $A_2 = 0.1$; $d_2/\lambda = 2.65$; $A_3 = 0.2$; $d_3/\lambda = 5$; N = 32; SF = 10

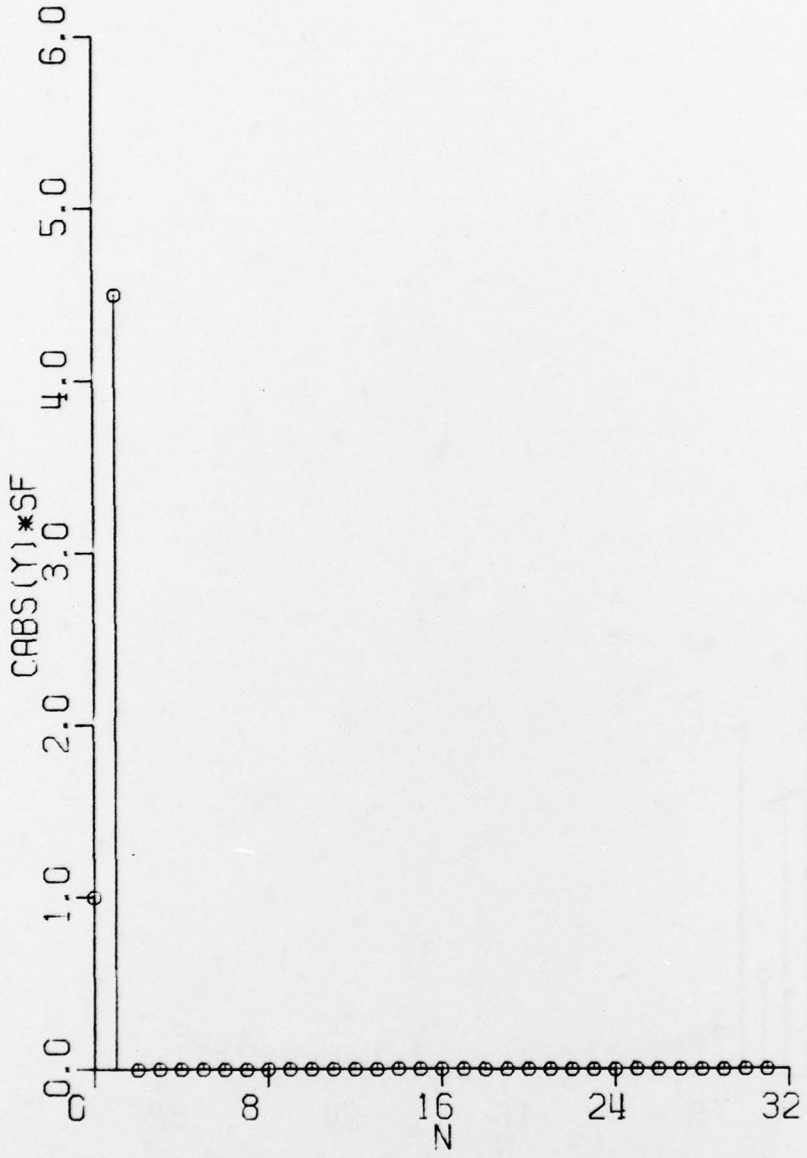

Fig. 37. Delay Determination: Noninteger Program
A = 0.45; d/λ = 3.5; N = 32; SF = 10

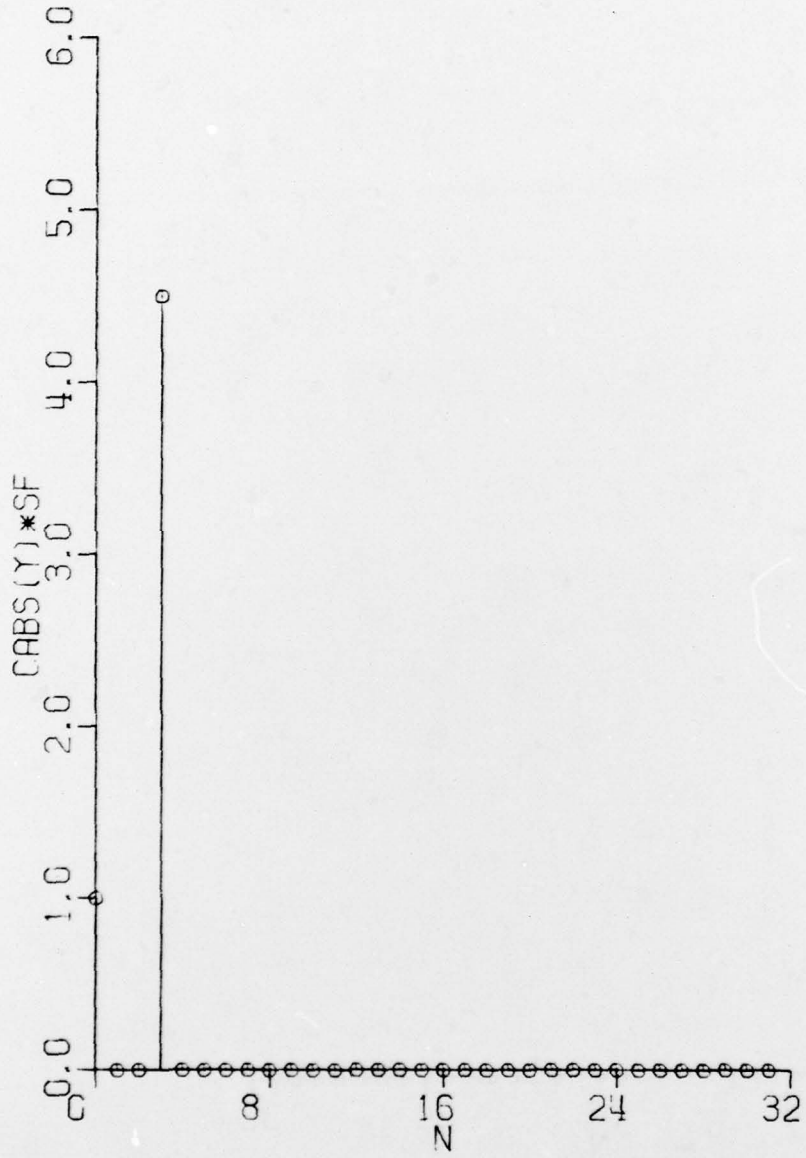

Fig. 38. Delay Determination: Noninteger Program
A = 0.45; d/λ = 10.5; N = 32; SF = 10

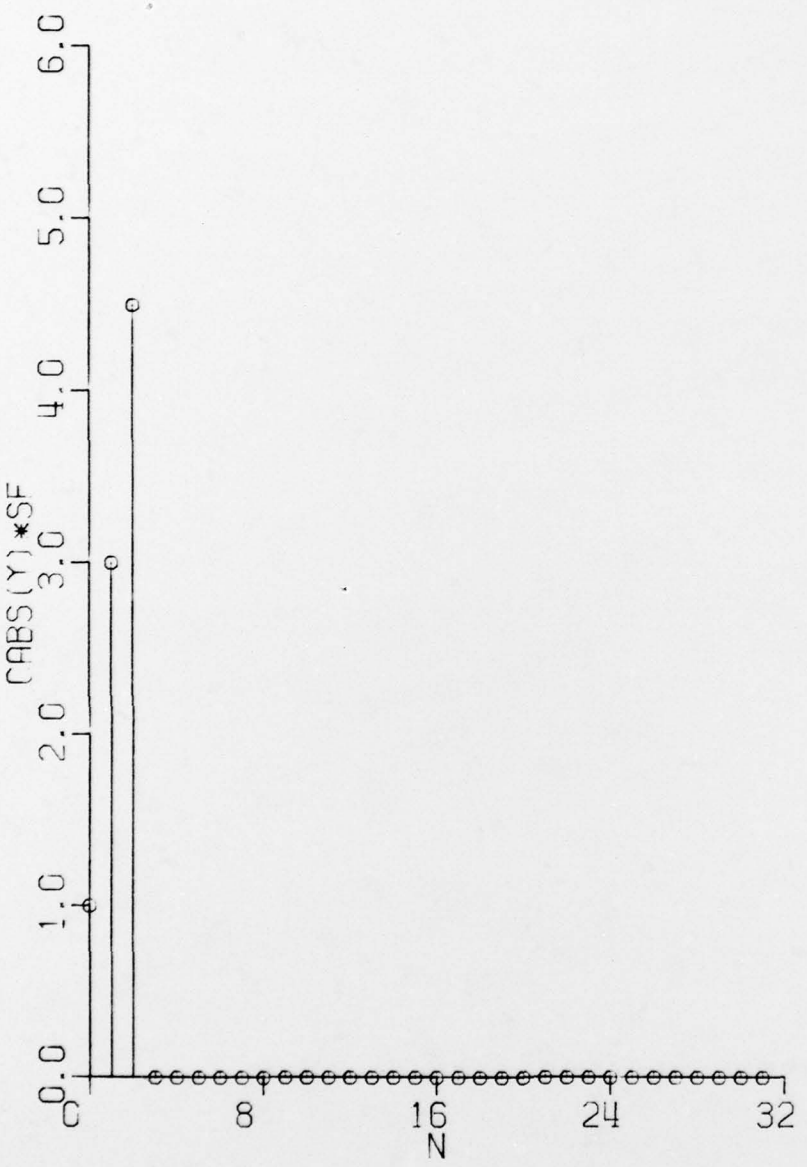

Fig. 39. Delay Determination: Noninteger Program
$A_1 = 0.3$; $d_1/\lambda = 1.25$; $A_2 = 0.45$; $d_2/\lambda = 2.5$; N = 32; SF = 10

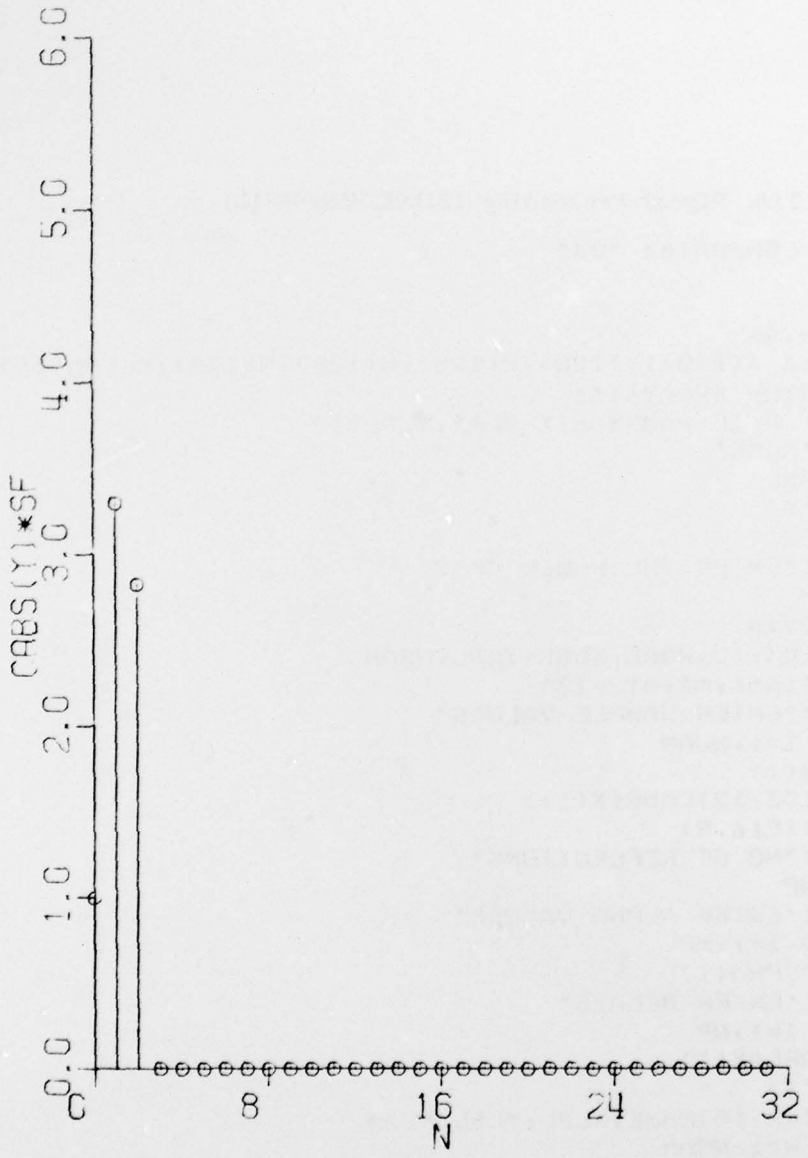

Fig. 40. Delay Determination: Noninteger Program
$A_1 = 0.33$; $d_1/\lambda = 1.25$; $A_2 = 0.2 + j0.2$; $d_2/\lambda = 2.5$;
$N = 32$; $SF = 10$

APPENDIX

Computer Program: Time Signal Processing (SILVERMAN/DRSIL)

```
10**RUN- * /RAMESH/DATA3 "03"
20C
30C
40        REAL MN,SF
50         COMPLEX X(128),Y(128),R(128),S(128),H(128),ALPHA(16)
60         DIMENSION DELAY(16)
70        CHARACTER IF,NAME*56,XLBL*1,YLBL*12
80      1 PRINT:"NAME"
90        READ:NAME
100        XLBL='N'
110        YLBL='X'
120        PRINT:"ENTER THE POWER OF 2"
130        READ:M
140        NSAM=2**M
150        WRITE(03,10)NAME,XLBL,YLBL,NSAM
160     10 FORMAT(A56,A1,A12,I3)
170        PRINT:"ENTER SAMPLE VALUES"
180        DO 20 I=1,NSAM
190        READ:X(I)
200     20 WRITE(03,12)CABS(X(I))
210     12 FORMAT(E16.8)
220        PRINT:"NO OF REFLECTIONS"
230        READ:NP
240        PRINT:"ENTER ALPHA VALUES"
250         DO 30 I=1,NP
260     30 READ:ALPHA(I)
270        PRINT:"ENTER DELAYS"
280        DO 40 I=1,NP
290     40 READ:DELAY(I)
300        YLBL='Y'
310        WRITE(03,10)NAME,XLBL,YLBL,NSAM
320        DO 60 N=1,NSAM
330        SUM=0
340        DO 50 I=1,NP
350        NT=N-DELAY(I)
360        IF(NT) 45,45,47
370     45  MN=0
380        GO TO 50
390     47 MN=ALPHA(I)*X(NT)
400     50 SUM=SUM+MN
410        Y(N)=X(N)+SUM
```

(SILVERMAN/DRSIL) continued

```
420    60 WRITE(03,12)CABS(Y(N))
430       PRINT:"X(N) VALUES ARE"
440       PRINT:(X(I),I=1,NSAM)
450       PRINT:"Y(N) VALUES ARE"
460       PRINT:(Y(N),N=1,NSAM)
470       CALL FFT(X,M)
480       CALL FFT(Y,M)
530       YLBL='H'
540       WRITE(03,10)NAME,XLBL,YLBL,NSAM
550       DO 70 I=1,NSAM
560       H(I)=EXP(-0.25*(I-1))
570    70 WRITE(03,12)CABS(H(I))
580       PRINT:"H VALUES ARE"
590       PRINT:(H(I),I=1,NSAM)
600       CALL FFT(H,M)
630       DO 80 I=1,NSAM
640       R(I)=X(I)*H(I)
650       X(I)=ABS(R(I))
660       X(I)=X(I)*X(I)
670       IF(X(I).EQ.0) X(I)=0.0000000001
680       X(I)=ALOG(X(I))
690       S(I)=Y(I)*H(I)
700       Y(I)=ABS(S(I))
710    80 Y(I)=ALOG(Y(I)*Y(I))
720       YLBL='X*H'
725       CALL INVFT(R,M)
730       WRITE(03,10)NAME,XLBL,YLBL,NSAM
740       WRITE(03,12)(CABS(R(I)),I=1,NSAM)
760       CALL INVFT(S,M)
770       YLBL='Y*H'
780       WRITE(03,10)NAME,XLBL,YLBL,NSAM
790       WRITE(03,12)(CABS(S(I)),I=1,NSAM)
800       CALL INVFT(X,M)
810       CALL INVFT(Y,M)
820       PRINT:"THE RESULTS ARE ..............."
830       YLBL='DL X 10'
840       WRITE(03,10)NAME,XLBL,YLBL,NSAM
850       DO 90 I=1,NSAM
860       X(I)=Y(I)-X(I)
870       WRITE(03,12)CABS(X(I)*10)
880    90 PRINT:X(I),I
930       PRINT:"FINISHED? ENTER 'YES' TO STOP, 'NO' TO CONTINUE"
940       READ:IF
950       IF(IF.EQ."NO") GO TO 1
960       STOP
970       END
```

(SILVERMAN/DRSIL) continued

```
      SUBROUTINE FFT(X,M)
      COMPLEX X(128),U,W,T
       N=2**M
       NV2=N/2
       NM1=N-1
       J=1
       DO 7 I=1,NM1
       IF(I.GE.J) GO TO 5
       T=X(J)
       X(J)=X(I)
       X(I)=T
    5  K=NV2
    6  IF(K.GE.J) GO TO 7
       J=J-K
       K=K/2
       GO TO 6
    7  J=J+K
       PI=3.14159265358979
       DO 20 L=1,M
       LE=2**L
       LE1=LE/2
       U=1.
       W=CMPLX(COS(PI/FLOAT(LE1)),-SIN(PI/FLOAT(LE1)))
       DO 20 J=1,LE1
       DO 10 I=J,N,LE
       IP=I+LE1
       T=X(IP)*U
       X(IP)=X(I)-T
   10  X(I)=X(I)+T
   20  U=U*W
       RETURN
       END
      SUBROUTINE INVFT(X,M)
C*X IS THE ARRAY CONTAINS THE TRANSFORM INITIALLY
C* AND FINALLY CONTAINS THE SEQUENCE.
      COMPLEX X(128),U,W,T
      N=2**M
      NV2=N/2
```

(SILVERMAN/DRSIL) continued

```
      NM1=N-1
      J=1
      DO 7 I=1,NM1
      IF(I.GE.J) GO TO 5
      T=X(J)
      X(J)=X(I)
      X(I)=T
    5 K=NV2
    6 IF(K.GE.J) GO TO 7
      J=J-K
      K=K/2
      GO TO 6
    7 J=J+K
      PI=3.14159265358979
      DO 20 L=1,M
      LE=2**L
      LE1=LE/2
      U=1.
      W=CMPLX(COS(PI/FLOAT(LE1)),SIN(PI/FLOAT(LE1)))
      DO 20 J=1,LE1
      DO 10 I=J,N,LE
      IP=I+LE1
      T=X(IP)*U
      X(IP)=X(I)-T
   10 X(I)=X(I)+T
   20 U=U*W
      FN=N
      DO 30 I=1,N
      X(I)=X(I)/FN
   30 CONTINUE
      RETURN
      END
```

Computer Program: Radiation Pattern Processing (NYAKA/CEPMLD)

```
10*$RUN= $ /RAMESH/DATA1 '03'
20       SUBROUTINE INVFT(X,M)
30C*X IS THE ARRAY CONTAINS THE TRANSFORM INITIALLY
40C* AND FINALLY CONTAINS THE SEQUENCE.
50       COMPLEX X(128),U,W,T
60       N=2**M
70       NV2=N/2
80       NM1=N-1
90       J=1
100       DO 7 I=1,NM1
110       IF(I.GE.J) GO TO 5
120       T=X(J)
130       X(J)=X(I)
140       X(I)=T
150    5  K=NV2
160    6  IF(K.GE.J) GO TO 7
170       J=J-K
180       K=K/2
190       GO TO 6
200    7  J=J+K
210       PI=3.14159265358979
220       DO 20 L=1,M
230       LE=2**L
240       LE1=LE/2
250       U=1.
260       W=CMPLX(COS(PI/FLOAT(LE1)),SIN(PI/FLOAT(LE1)))
270       DO 20 J=1,LE1
280       DO 10 I=J,N,LE
290       IP=I+LE1
300       T=X(IP)*U
310       X(IP)=X(I)-T
320   10  X(I)=X(I)+T
330   20  U=U*W
340       FN=N
350       DO 30 I=1,N
360       X(I)=X(I)/FN
370   30  CONTINUE
380       RETURN
390       END
400       SUBROUTINE PATTN(E,X)
410C*THIS COMPUTES FIELD PATTERN AT ANGLES PHI
420       COMMON A,DL,M,NR
430       INTEGER M,NR,KI
```

(NYAKA/CEPMLD)

```
      REAL X(128),DL(10)
      COMPLEX A(10),E(128),ESKI
      N=2**M
      PI=3.14159265358979
      DO 20 I=1,N
      E(I)=CMPLX(1.0,0.0)
      DO 10 K=1,NR
      KI=K*I
      BKI=2.0*PI*DL(K)*X(I)
      ESKI=A(K)*CMPLX(COS(BKI),-SIN(BKI))
      E(I)=E(I)+ESKI
10    CONTINUE
20    CONTINUE
      RETURN
      END
C      MAIN PROGRAM
1     PRINT:"#"
      READ:NUMBER
      PRINT:"                          PLOT #",NUMBER
      COMMON A,DL,M,NR
      REAL Z(128),R(128),X(128),DL(10),SF
      COMPLEX A(10),E(128),Y(128)
      CHARACTER IF,NAME*56,XLBL*1,YLBL*12
      PRINT:"N=2**M; ENTER 'M' "
      READ:M
      N=2**M
      PRINT:"# OF REFLECTIONS"
      READ:NR
      PRINT:"VALUE OF L"
      READ:L
      IF(L) 25,22,25
22    L=N
25    DO 30 I=1,N
      XM=I-1
      X(I)=XM/L
30    CONTINUE
      PRINT:"VALUES OF A(I)?"
      DO 31 J=1,NR
31    READ:A(J)
      PRINT:"VALUES OF DL(I)?"
      DO 32 J=1,NR
```

(NYAKA/CEPMLD) continued

```
      READ:DL(J)
      CALL PATTN(E,X)
      DO 33 I=1,N
      IL=I
33    CONTINUE
      DO 35 I=1,N
      IL=I
      Y(I)=E(I)
35    CONTINUE
      CALL INVFT(Y,M)
      PRINT:"SCALE FACTOR"
      READ:SF
C*Y(I) WILL BE FINAL SEQUENCE OF COMPOSITE FIELD
      XLBL="N"
      YLBL="CABS(Y)*SF"
      PRINT:"NAME"
      READ:NAME
      WRITE(03,37) NAME,XLBL,YLBL,N
37    FORMAT(A56,A1,A12,I3)
       DO 40 I=1,N
       IN=I
       PRINT:(IN-1),CABS(Y(IN)),Y(IN)
       YIN=CABS(Y(IN))
       IF(YIN-0.5) 38,38,39
38     YIN=YIN*SF
39     WRITE(03,45) YIN
45     FORMAT(E16.8)
40     CONTINUE
       PRINT:"FINISHED? ENTER 'YES' TO STOP, 'NO' TO CONTINUE"
       READ:IF
       IF(IF.EQ."NO") GO TO 1
       STOP
       END
```

Computer Program: Plotter Routine (RAMESH/PLTCP3)

```
1$$N,J
20$       IDENT   BLA00001,PERINI-RM,956700160121,PLTCP3
30$       OPTION  FORTRAN
40$       FORTY
50       DIMENSION X(500),Y(500)
60       CHARACTER NAME*56,XLBL*1,YLBL*12,USER*9
70       CALL INITAL(26,500,12,1,0,0)
80       USER='PERINI-NY'
90 101   READ(03,1,END=100) NAME,XLBL,YLBL,N
100  1    FORMAT(A56,A1,A12,I3)
110       READ(03,3) (Y(I),I=1,N)
120  3    FORMAT(E16.8)
130       CALL RSTR(2)
140       XAXIS=N*0.125
150       YAXIS=6.0
160       CALL PLOT(2.0,2.5,-3)
170       CALL SYMBOL(-1.0,-2.0,.56,USER,90.0,9)
200       CALL AXIS(0.,0.,XLBL,-1,XAXIS,0.,0.,8.0,-1)
210       CALL AXIS(0.,0.,YLBL,+12,YAXIS,90.,0.,1.0,1)
215       CALL PLOT(0.,Y(1),3)
216       CALL MARKER(1)
217       CALL PLOT(0.,0.,2)
220       DO 10 I=2,N
223       X(I)=0.125*(I-1)
224       CALL PLOT(X(I),Y(I),3)
225       CALL MARKER(1)
226       CALL PLOT(X(I),0.,2)
227  10   X(I)=X(I)+0.125
230       CALL SYMBOL(-.75,-2.0,.14,NAME,0.0,56)
240       GO TO 101
250  100  CALL RSTR(2)
260       STOP
270       END
280$       SELECT  LIBRARY/COMPLOT
290$       EXECUTE
300$       MSG2    1,PLEASE RUN TAPE THROUGH PLOTTER
310$       MSG2    1,AT COMPLETION OF THIS JOB
320$       LIMITS  30,20K,,,
330$       FFILE   26,NSTDLB,NOSRLS,FIXLNG/226,NOSLEW,BUFSIZ/226
340$       TAPE9   26,X1D,,16725,,SUPLOT-SW,,DEN8
350$       PRMFL   03,R/W,S,BLA00001/RAMESH/DATA3
360$       ENDJOB
```

MISSION
of
Rome Air Development Center

RADC plans and executes research, development, test and selected acquisition programs in support of Command, Control Communications and Intelligence (C^3I) activities. Technical and engineering support within areas of technical competence is provided to ESD Program Offices (POs) and other ESD elements. The principal technical mission areas are communications, electromagnetic guidance and control, surveillance of ground and aerospace objects, intelligence data collection and handling, information system technology, ionospheric propagation, solid state sciences, microwave physics and electronic reliability, maintainability and compatibility.